Article

Cell Metabolism

CRFR1 in AgRP Neurons Modulates Sympathetic Nervous System Activity to Adapt to Cold Stress and Fasting

Graphical Abstract

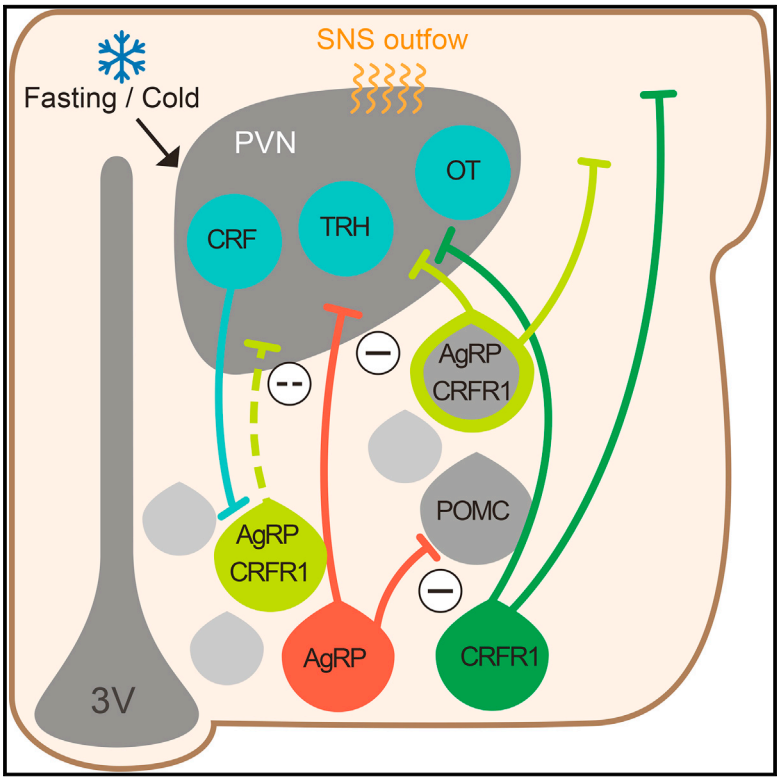

Highlights

- Stress regulation and energy balance share common hypothalamic neurocircuits
- Adaptive transition to catabolic state requires CRFR1 signaling in AgRP neurons
- CRFR1 signaling negates AgRP neuronal action by reducing their excitability
- CRFR1 signaling in AgRP neurons is required for coping with environmental challenges

Authors

Yael Kuperman, Meira Weiss, Julien Dine, ..., Jan M. Deussing, Matthias Eder, Alon Chen

Correspondence

yael.kuperman@weizmann.ac.il (Y.K.), alon.chen@weizmann.ac.il (A.C.)

In Brief

Kuperman et al. reveal a critical role for the stress-induced CRF receptor expressed in a subset of AgRP neurons in females. CRF receptor activation following challenge reduces AgRP neuronal excitability and enables appropriate sympathetic nervous system activation, thereby protecting the organism from hypothermia and hypoglycemia.

Kuperman et al., 2016, Cell Metabolism *23*, 1185–1199
June 14, 2016
http://dx.doi.org/10.1016/j.cmet.2016.04.017

CellPress

Cell Metabolism
Article

CRFR1 in AgRP Neurons Modulates Sympathetic Nervous System Activity to Adapt to Cold Stress and Fasting

Yael Kuperman,[1,*] Meira Weiss,[2,3] Julien Dine,[3] Katy Staikin,[2,3] Ofra Golani,[4] Assaf Ramot,[2,3] Tali Nahum,[2] Claudia Kühne,[3] Yair Shemesh,[2,3] Wolfgang Wurst,[5] Alon Harmelin,[1] Jan M. Deussing,[3] Matthias Eder,[3] and Alon Chen[2,3,*]
[1]Department of Veterinary Resources, Weizmann Institute of Science, 76100 Rehovot, Israel
[2]Department of Neurobiology, The Ruhman Family Laboratory for Research on the Neurobiology of Stress, Weizmann Institute of Science, 76100 Rehovot, Israel
[3]Department of Stress Neurobiology and Neurogenetics, Max Planck Institute of Psychiatry, 80804 Munich, Germany
[4]Biological Services Unit, Weizmann Institute of Science, 76100 Rehovot, Israel
[5]Helmholtz Zentrum München, German Research Center for Environmental Health, Institute of Developmental Genetics, 85764 Neuherberg, Germany
*Correspondence: yael.kuperman@weizmann.ac.il (Y.K.), alon.chen@weizmann.ac.il (A.C.)
http://dx.doi.org/10.1016/j.cmet.2016.04.017

SUMMARY

Signaling by the corticotropin-releasing factor receptor type 1 (CRFR1) plays an important role in mediating the autonomic response to stressful challenges. Multiple hypothalamic nuclei regulate sympathetic outflow. Although CRFR1 is highly expressed in the arcuate nucleus (Arc) of the hypothalamus, the identity of these neurons and the role of CRFR1 here are presently unknown. Our studies show that nearly half of Arc-CRFR1 neurons coexpress agouti-related peptide (AgRP), half of which originate from POMC precursors. Arc-CRFR1 neurons are innervated by CRF neurons in the hypothalamic paraventricular nucleus, and CRF application decreases $AgRP^{+}CRFR1^{+}$ neurons' excitability. Despite similar anatomy in both sexes, only female mice selectively lacking CRFR1 in AgRP neurons showed a maladaptive thermogenic response to cold and reduced hepatic glucose production during fasting. Thus, CRFR1, in a subset of AgRP neurons, plays a regulatory role that enables appropriate sympathetic nervous system activation and consequently protects the organism from hypothermia and hypoglycemia.

INTRODUCTION

The well-being of an organism necessitates appropriate physiological responses to homeostatic challenges. The hypothalamus integrates neural circuits for control of survival behaviors, including feeding, drinking, defense, and reproduction (Sternson, 2013). These circuits often intertwine and overlap and are regulated by various neurotransmitters and neuropeptides. Hypothalamic corticotropin-releasing factor (CRF; also known as corticotropin-releasing hormone [CRH]), secreted from the parvocellular neurons in the paraventricular nucleus (PVN), has a prominent role in initiating the cascade of biological events during the stress response and represents a neuropeptide that affects a vast repertoire of the aforementioned behaviors. CRF's physiological actions are mediated primarily by activating the CRF receptor type 1 (CRFR1/CRHR1), which is required for appropriate behavioral and neuroendocrine responses to stress (Müller et al., 2003; Smith et al., 1998; Timpl et al., 1998). CRFR1 is widely expressed in the mammalian brain with high expression levels in the cerebral cortex, amygdala, hippocampus, olfactory bulb, and hypothalamic arcuate nucleus (Arc) (Van Pett et al., 2000). Early upon CRF isolation (Vale et al., 1981), it was shown that in addition to its hypophysiotrophic role, CRF acts within the brain to stimulate sympathetic outflow. This was manifested by elevated heart rate and mean arterial pressure (Fisher et al., 1982) as well as increases in blood glucose, norepinephrine, epinephrine, and glucagon levels (Brown et al., 1982). These hormonal changes were associated with increases in motor activity and oxygen consumption and were attributed to the central action of CRF, as they were not prevented by adrenalectomy (Brown et al., 1982). Later studies using selective antagonists were able to confirm that stress-induced norepinephrine release is mediated by CRFR1 activation (Griebel et al., 2002). Consistent with this, CRF involvement in adaptive thermogenesis was also demonstrated. Intracerebroventricular administration of CRF stimulates sympathetic outflow to brown adipose tissue (BAT) (Arase et al., 1988). This action was suggested to be mediated through CRF receptors in the dorsomedial hypothalamus (DMH) as well as the preoptic area (Cerri and Morrison, 2006), whereas the effect through PVN-CRFR was questionable (Cerri and Morrison, 2006; LeFeuvre et al., 1987).

Several hypothalamic nuclei were shown to regulate autonomic responses to stressors (Ulrich-Lai and Herman, 2009), of which the PVN is prominent. Within the PVN, distinct sympathetic premotor neurons project to either the sympathetic intermediolateral nucleus of the spinal cord or the parasympathetic dorsal vagal motor nucleus (Swanson and Sawchenko, 1980; Viñuela and Larsen, 2001). Retrograde tracing showed forebrain neurons innervating the BAT, which arise mainly from the PVN and the medial preoptic region (mPO) and to a lesser extent from the ventromedial hypothalamus (VMH) and the lateral

hypothalamus (LH) and the suprachiasmatic nucleus (SCN) (Bamshad et al., 1999). Likewise, retrograde tracing from the liver labeled second-order neurons in several regions, including the PVN, LH, zona incerta, and retrochiasmatic area (la Fleur et al., 2000).

The PVN is heavily innervated by GABAergic inputs, which deliver substantial inhibitory tone important for regulating sympathetic outflow. Antagonizing PVN GABAergic receptors increases sympathetic nerve activity (Cole and Sawchenko, 2002; Kannan et al., 1989; Madden and Morrison, 2009). Intra-hypothalamic sources for GABAergic input to the PVN include the mPO, DMH, LH, SCN, and Arc (Cone, 2005; Herman et al., 2005; Kalsbeek et al., 2004), as well as GABAergic interneurons in the halo zone surrounding the PVN, including the anterior hypothalamic and perifornical regions (Roland and Sawchenko, 1993).

The Arc is composed of two main populations of neurons, neuroendocrine neurons that have nerve endings in the median eminence and neurons regulating energy homeostasis (Lehman et al., 2013). The appetite-regulatory network in the Arc includes two major distinct populations with opposing actions on food intake and metabolic rate: the anorexigenic pro-opiomelanocortin (POMC) neurons and the orexigenic agouti-related peptide (AgRP) neurons, which coexpress neuropeptide-Y (NPY) and γ-aminobutyric acid (GABA) (Cone, 2005).

Despite the high expression level, the identity of Arc-CRFR1 neurons and the role of CRFR1 in this brain region are presently unknown. Here, we show that CRFR1 marks a unique subpopulation of AgRP neurons, half of which originate from POMC precursor. This subpopulation projects predominantly to regions associated with regulation of food intake and autonomic outflow. We show that CRF decreases the excitability of neurons immunopositive for both AgRP and CRFR1 ($AgRP^+CRFR1^+$) and that under challenge, CRFR1 signaling in these neurons helps the organism transition from an anabolic to a catabolic state in order to promote survival.

RESULTS

CRFR1 Marks a Subpopulation of AgRP Neurons, Some of which Originate from POMC Precursors

To characterize CRFR1-expressing neurons in the Arc, we used the well-validated *CRFR1-GFP* reporter mouse (Justice et al., 2008). This mouse line is based on a bacterial artificial chromosome that contains the entire CRFR1 genomic locus and has GFP cellular expression that closely matches that of *Crfr1* mRNA (Justice et al., 2008). We further examined the Arc of these mice, validating that the *Gfp* expression matches that of *Crfr1* by double in situ hybridization (Figure 1A). To explore the colocalization of CRFR1 with AgRP-expressing neurons, we crossed the *CRFR1-GFP* mouse with an AgRP reporter mouse, which expresses Cre recombinase under control of the AgRP promoter (*AgRP-IRES-Cre*; Tong et al., 2008) and a reporter allele encoding tdTomato red fluorescent protein upon Cre-mediated recombination (*Rosa26-CAG-lsl-tdtomato, Ai9*; Madisen et al., 2010). Analysis of Arc sections obtained from these mice (*CRFR1-GFP-AgRP*^{TOM}) showed that half of Arc-CRFR1 neurons colocalize with AgRP-expressing neurons (males, 46.7 ± 5.7%; females, 50.4 ± 5.0%), defining half of AgRP neurons (males 52.6 ± 9.9%; females 50.4 ± 8.5%) (Figures 1B and 1H). We found that the numbers of CRFR1 and AgRP neurons are similar and do not significantly differ between males and females (Figure S1A). In addition, we found that the expression levels of *Agrp* and *Crfr1*in the mediobasal hypothalamus (MBH) of wild-type (WT) mice does not differ between males and females (Figure S1B). We further assessed whether CRFR1 colocalizes with POMC-expressing neurons by crossing the *CRFR1-GFP* with mice expressing Cre recombinase specifically in POMC-expressing neurons or cells (*POMC-Cre*; Balthasar et al., 2004) and the Tomato reporter (*CRFR1-GFP-POMC*^{TOM} mice). Analysis of Arc slices obtained from these mice revealed that about a third of Arc-CRFR1 neurons colocalize with *POMC-Cre*-expressing neurons (31.7 ± 3.15%; Figures 1C and 1H). Given that *POMC-Cre* marks not only adult POMC-expressing neurons but also POMC neurons that transdifferentiated from a POMC precursor during early developmental stages (Padilla et al., 2010, 2012), we further used immunohistochemistry (IHC) for adrenocorticotropic hormone (ACTH), which is processed from the POMC precursor and therefore marks neurons currently expressing POMC. ACTH immunostaining showed that in adult mice, CRFR1 and ACTH do not colocalize (Figure 1D).

We further explored the colocalization of CRFR1 with rat insulin promoter (RIP)-Cre-, dopamine-, and somatostatin (SST)-expressing neurons. We found that 36 ± 1.9% and 17.1 ± 1.3% of Arc CRFR1 neurons colocalize with RIP-Cre- and SST-expressing neurons, respectively (Figures 1E and 1F), whereas no colocalization was observed with dopaminergic neurons (Figure 1G).

The finding that in adult mice, CRFR1 and ACTH are expressed in a mutually exclusive manner suggests that CRFR1 marks a subpopulation of POMC neurons that adopt a non-POMC fate (Figure 2A). Because about a quarter of the Arc-NPY population originates from a POMC progenitor (Padilla et al., 2010) we further assessed whether POMC-Cre^+CRFR1^+ neurons adopted an AgRP fate by using IHC for AgRP on slices obtained from *CRFR1-GFP-POMC*^{TOM} mice. This indicated that the majority of POMC-Cre^+CRFR1^+ neurons express AgRP, signifying that CRFR1 marks POMC neurons that adopt an AgRP fate (Figure 2B, white arrows). Importantly, POMC-Cre^+ $AgRP^+CRFR1^-$ neurons were rarely found (Figure 2B, gray arrow).

To rule out the possibility that absence of CRFR1 affects the early embryonic shift of POMC cells, we measured POMC and AgRP expression levels in hypothalami obtained from developmental CRFR1 knockout (KO) mice. CRFR1 KO mice are glucocorticoid (GC) deficient (Smith et al., 1998); therefore, in order to avoid effects mediated by the absence of circulating GC, we collected hypothalami of CRFR1 KO and their WT littermates at postnatal day 4, while the pups receive GC from their mother's milk. No differences in *Agrp* or *Pomc* mRNA expression levels were observed in CRFR1 KO (Figure 2C).

In summary, Arc-CRFR1 is expressed by at least three neuronal populations (SST, AgRP, and RIP), which share inhibitory properties (Bluet-Pajot et al., 1998; Kong et al., 2012; Wu et al., 2009) (Figure 1D). Most of Arc-CRFR1 is expressed by orexigenic neurons, the major population being AgRP-expressing neurons. Because not all $AgRP^+CRFR1^+$ express the POMC-Cre lineage marker, we suggest that $AgRP^+CRFR1^+$ neurons arise from at least two ontological lineages.

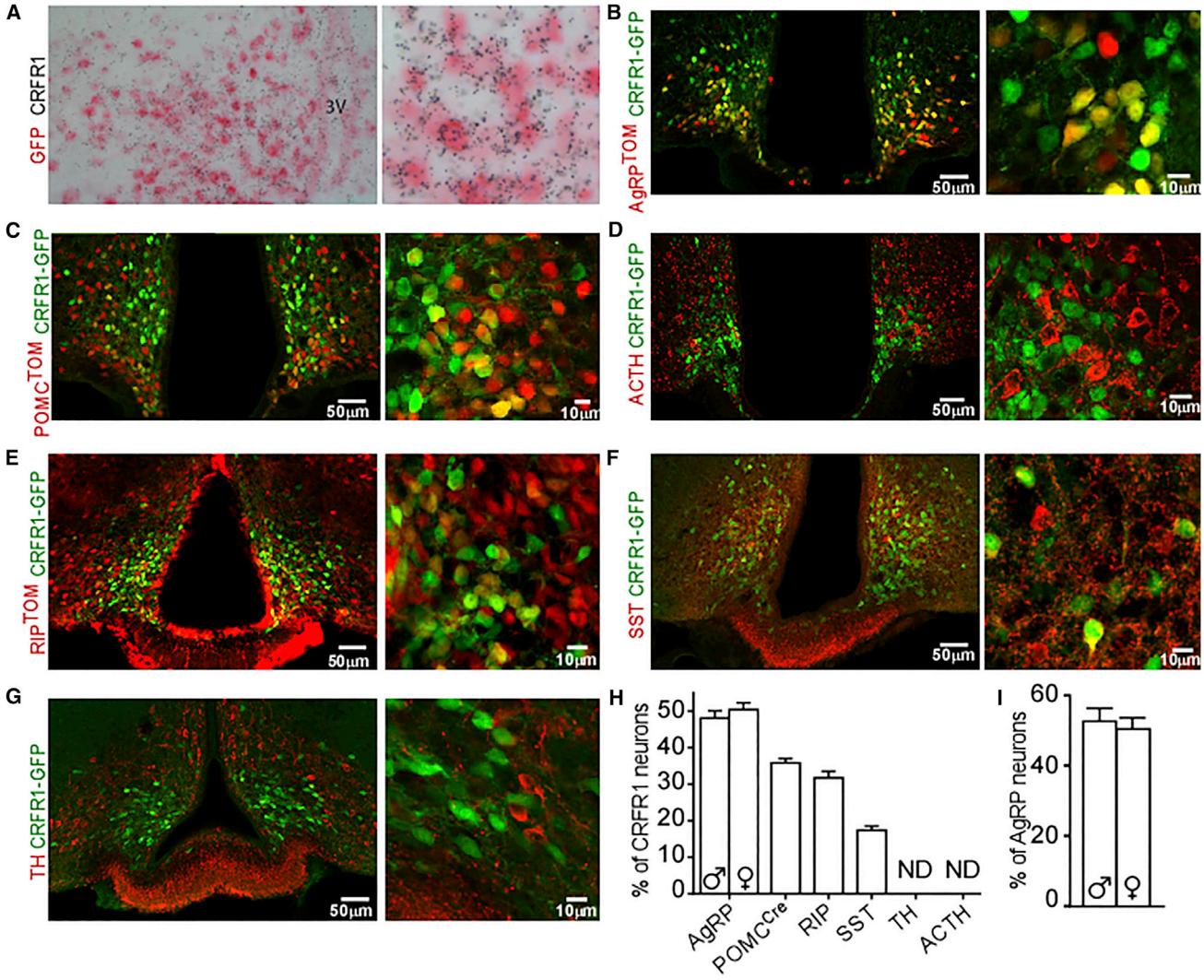

Figure 1. CRFR1 in the Arc Is Expressed in Neurons Regulating Food Intake and Growth

(A) Double in situ hybridization for *Crfr1* and *Gfp* on *CRFR1-GFP* mice.

(B) Immunodetection of GFP in the Arc of *CRFR1-GFP* mice crossed with AgRP reporter mice (*CRFR1-GFP-AgRP*^{TOM}).

(C) Immunodetection of GFP and AgRP in the Arc of colchicine injected *CRFR1-GFP* mice crossed with POMC reporter mice (*CRFR1-GFP-POMC*^{TOM}).

(D) Immunodetection of GFP and ACTH in the Arc of *CRFR1-GFP* mice.

(E) Immunodetection of GFP in the Arc of *CRFR1-GFP* mice crossed with RIP reporter mice (*CRFR1-GFP-RIP*^{TOM}).

(F) Immunodetection of GFP and SST in the Arc of colchicine injected *CRFR1-GFP* mice.

(G) Immunodetection of GFP and TH in the Arc of colchicine injected *CRFR1-GFP* mice.

(H) Percentage of each CRFR1 subpopulation from total Arc-CRFR1-expressing neurons. Values are mean ± SEM. ND, not detected. AgRP n = 7 for each sex; POMC-Cre n = 3; ACTH n = 2; RIP n = 2; SST n = 2; TH n = 2.

(I) Percentage of CRFR1 subpopulation from total AgRP-expressing neurons. Values are mean ± SEM (n = 7 for each sex).

AgRP-CRFR1 Neurons Respond to Known AgRP Stimulants

To deepen the characterization of AgRP^{+}CRFR1^{+} neurons, we checked their responsiveness to different physiological and hormonal signaling. Using the *CRFR1-GFP-AgRP*^{TOM} reporter mice we verified that as reported for AgRP neurons, AgRP^{+}CRFR1^{+} neurons are activated by fasting and by ghrelin, measured by the expression of the early mediated gene, *c-fos* (Liu et al., 2012; Wang et al., 2002). Indeed, *c-fos* expression was upregulated in AgRP neurons following a 24 hr fast or following ghrelin injection compared with fed mice or saline-injected mice, respectively, regardless of CRFR1 expression (Figures S1C and S1D).

About one third of AgRP neurons were reported to respond to leptin injection as marked by phosphorylation of signal transducer and activator of transcription 3 (STAT3; van de Wall et al., 2008).

IHC with pSTAT3 antibody on slices obtained from the double-reporter mice injected with leptin revealed that a third of CRFR1 neurons respond to leptin in both males and females (Figures 2D and 2E). Leptin-responsive AgRP neurons were evenly distributed in AgRP^{+}CRFR1^{+} and in AgRP^{+}CRFR1^{-}

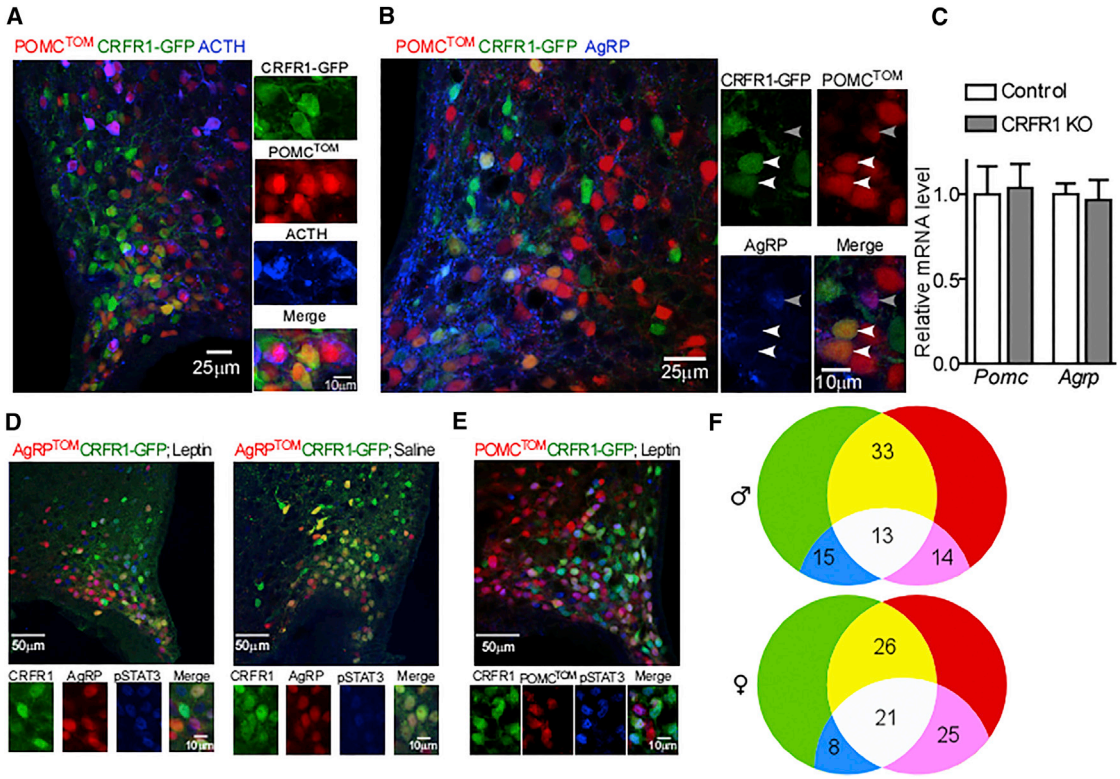

Figure 2. CRFR1 Marks AgRP Neurons Originating from POMC Precursor

(A) Immunodetection of GFP and ACTH in the Arc of colchicine injected *CRFR1-GFP* mice crossed with POMC reporter mice (*CRFR1-GFP-POMC*^{TOM}).

(B) Immunodetection of GFP and AgRP in the Arc of colchicine injected *CRFR1-GFP* mice crossed with POMC reporter mice (*CRFR1-GFP-POMC*^{TOM}).

(C) *Pomc* and *Agrp* relative expression in 4-day-old CRFR1 KO mice and their WT littermates (n = 4 or 5).

(D) Immunodetection of pSTAT3 in the Arc of leptin- or saline-injected, overnight-fasted *CRFR1-GFP-AgRP*^{TOM} reporter mice.

(E) Immunodetection of pSTAT3 in the Arc of leptin-injected, overnight-fasted *CRFR1-GFP-POMC*^{TOM} reporter mice.

(F) Venn diagrams displaying the percentage of unique and overlapping leptin responsive CRFR1 and AgRP neurons in males and females (n = 3 for each sex). See also Figure S1E.

neurons. AgRP leptin responsiveness tended to be higher in females compared with males (females, 46.2% ± 1.2%; males, 32.4% ± 10.2%; p = 0.08; Figure 2F and Figure S1E), supporting the suggested increased leptin signaling in the Arc of females (Clegg et al., 2003). The percentage of AgRP$^+$CRFR1$^+$ neurons that were responsive to leptin was similar to that of total AgRP. This suggests that within each sex, leptin-responsive AgRP neurons were evenly distributed in AgRP$^+$CRFR1$^+$ and in AgRP$^+$CRFR1$^-$ neurons. This was supported by a similarly responsive population within POMC-Cre$^+$CRFR1$^+$ neurons (Figures 2D and 2E and Figure S1E).

AgRP-CRFR1 Neurons Project Mainly to the LH and the PVN and Are Innervated by PVN-CRF Neurons

AgRP neurons project to a number of brain areas covering both rostral and caudal regions (Broberger et al., 1998). AgRP projections to different brain regions were shown to originate from separate, distinct subpopulations of AgRP neurons (Betley et al., 2013). Because CRFR1 marks a subset of AgRP neurons, we wondered whether this population has a distinct projection profile. For this purpose, we used the double-reporter mice and characterized the projections of AgRP$^+$CRFR1$^+$ neurons. Nine AgRP projection fields were analyzed, and the proportion of AgRP$^+$CRFR1$^+$ projections out of total AgRP projections to each region was quantified using IMMARIS software. AgRP$^+$CRFR1$^+$ neurons were found to project mainly to the LH, the PVN, the periaqueductal gray (PAG), and the bed nucleus of the stria terminalis (BNST) (Figure 3A). Weaker projections were observed at the DMH, the mPO, the paraventricular thalamic nucleus (PVT), the central amygdala (CeA), and the parabrachial nucleus (PBN) (Figure S2). Overall, AgRP$^+$CRFR1$^+$ projections were found to constitute between 2% and 14% of AgRP projections to the inspected regions (Figure 3B, left y axis). Importantly, this analysis underestimates the overlapping projections because of strict analysis criteria that were used in order to distinguish regional CRFR1 projections from AgRP$^+$CRFR1$^+$ projections. The intensity of AgRP projection varies in different brain regions (Wang et al., 2015). Therefore, the proportion of AgRP$^+$CRFR1$^+$ projections was calculated according to the relative portion of AgRP neurons projection to a specific site (raw data taken from experiment 46554676-Arc, Allen Mouse Brain Connectivity Atlas [Oh et al., 2014]; Figures 3B, right y axis, and 3C). Interestingly, within the PVN, and in agreement with AgRP inhibitory action on sympathetic outflow, we could detect AgRP$^+$CRFR1$^+$ neurons innervating PVN-TH$^+$ neurons (Figure 3D, white arrows).

Another intriguing question regarding the connectivity of AgRP^{+}CRFR1^{+} neurons is the origin and identity of the CRFR1 ligand. From the mammalian CRF peptide family (Lewis et al., 2001; Reyes et al., 2001; Vaughan et al., 1995), both CRF and urocortin 1 (Ucn1) are potential nominees for innervating Arc-CRFR1 neurons. In order to check whether CRF innervates AgRP^{+}CRFR1^{+} neurons, we searched for CRF positive synapses, marked by post-synaptic density 95 (PSD95) in AgRP reporter mice. Confocal analysis verified that endogenous CRF innervates AgRP neurons (Figures 3D and 3E, white arrow). CRF is expressed in diverse brain regions, including the cortex, hippocampus, and CeA (Swanson et al., 1983). Yet the immediate candidate for Arc-CRFR1 neurons innervations is CRF arising from the PVN, either directly or as collaterals of CRF neurons projecting to the median eminence (Niimi et al., 1988). To examine this hypothesis, we injected a viral vector encoding a Cre-dependent mCherry reporter fused to synaptophysin into the PVN of *CRF-Cre* mice (Taniguchi et al., 2011), which were crossed with *CRFR1-GFP* mice. In these mice, red synapses represent synapses in which the pre-synaptic neurons are PVN-CRF-expressing neurons. Confocal analysis confirmed that Arc-CRFR1 neurons are innervated by CRF neurons arising from the PVN (Figure 3F). We do not rule out the possibility that Arc-CRFR1 neurons could also be innervated by Ucn1 or by CRF arising from other brain regions.

CRF Application Decreases AgRP Neurons' Excitability

To determine the significance of CRFR1 signaling in AgRP neurons in regulating energy homeostasis, we generated mice lacking CRFR1 specifically in AgRP neurons (AgRPΔCRFR1; Figure 4A). CRFR1 deletion was confirmed by quantitative real-time PCR analysis showing, as expected, a 40% reduction in *Crfr1* expression levels in the MBH of AgRPΔCRFR1 mice (Figure 4B). The reduction in *Crfr1* expression is consistent with the confocal analysis showing that 50% of CRFR1 neurons co-localize with AgRP neurons (Figure 1B). To ensure the restricted CRFR1 deletion in the Arc of AgRPΔCRFR1 mice, we verified that *Crfr1* expression was unchanged in several brain regions with high *Crfr1* expression (Figure S3A). *Crfr1* mRNA level was also similar in peripheral tissues that were described for developmental AgRP expression (Figure S3A). In addition, we confirmed that pituitary *Crfr1* expression level and both basal and stress-induced hypothalamic-pituitary-adrenal (HPA) axis function was intact in AgRPΔCRFR1 mice (Figures S3B and S3C). This is in line with mice lacking CRFR1 from GABAergic neurons that exhibit intact HPA function and no changes in anxiety-like behavior (Refojo et al., 2011).

We crossed AgRPΔCRFR1 mice with *CRFR1-GFP-AgRP*^{TOM} mice to generate mice in which AgRP^{+}CRFR1^{+} neurons are labeled but do not express CRFR1. Then, to define whether and how the electrophysiological properties of AgRP neurons are modulated by CRF, we visually identified AgRP^{+}CRFR1^{+} neurons in acute Arc brain slices (Figure S3D) and performed patch-clamp recordings in these cells in slices obtained from both female and male double-reporter mice with (control) or without (AgRPΔCRFR1) CRFR1 expression.

Acute activation of the stress response and AgRP stimulation has opposing effects regarding food intake and autonomic activity. Therefore, we hypothesize that, similar to leptin (van den Top et al., 2004), CRF action on AgRP^{+}CRFR1^{+} neurons will have an inhibitory effect, negating the typical nature of AgRP neurons. Firing of action potentials (APs) was evoked in AgRP^{+}CRFR1^{+} neurons by current injection under control conditions and after bath application of CRF (125 nM). Remarkably, CRF application strongly decreased evoked neuronal firing (Figure 4C, left). This effect was mediated by CRFR1 activation, as it was completely abolished in AgRPΔCRFR1 mice (Figure 4C, right). Concomitant with the decrease in neuronal excitability, the after-hyperpolarization (AHP) was increased by CRF application (Figure 4D, left). This increase in AHP amplitude could explain the CRF-mediated decrease in firing rate, implicating that AgRP^{+}CRFR1^{+} neurons require a longer time to repolarize after generating an AP, thus delaying the appearance of another AP. However, this effect cannot explain the total absence of APs in the presence of CRF, which was observed in some cells (Figure 4C, left). Consistently, we revealed that CRF additionally reduced the input resistance (R_{in}) of AgRP neurons (Figure 4E, left). This effect and the increase in AHP amplitude were absent in AgRPΔCRFR1 mice (Figures 4D and 4E, right).

Notably, CRF application had no effect on AgRP-positive neurons (tdTomato positive), which do not express CRFR1 (GFP negative; Figures S3E and S3F). This further supports the observed effects as direct and specific for AgRP^{+}CRFR1^{+} neurons.

CRFR1 Signaling in AgRP Neurons Regulates Heat Production

Given the inhibitory tone CRF poses on AgRP neurons and the projection profile of AgRP^{+}CRFR1^{+} neurons, we postulated that in the absence of CRFR1, AgRP neurons will have higher activity, leading to stronger suppression of the target regions. This could result in increased food intake and reduced energy expenditure. We followed the body weight and growth rates of both male and female AgRPΔCRFR1 mice and found them similar to that of their control littermates (Figure 5A). In line with the similar body weight, AgRPΔCRFR1 mice did not differ in their body composition and had similar percentages of fat and lean masses (Figures S4A and S4B). Glucose and insulin tolerance tests revealed no disturbance in glucose homeostasis or insulin sensitivity in AgRPΔCRFR1 mice on standard diet (Figures S4C–S4F). Food intake of AgRPΔCRFR1 mice was equivalent to their control littermates, and their feeding response to ghrelin injection was intact (Figures S5A and S5B). This suggests that despite projecting to brain regions associated with the orexigenic action of AgRP, CRFR1 signaling in AgRP^{+}CRFR1^{+} neurons does not modulate feeding directly.

Interestingly, although they have similar food intake and locomotor activity (Figures S5A and S5C), AgRPΔCRFR1 female mice exhibited reduced heat production during the dark phase of the day cycle (Figure 5B). The reduced heat production was reflected in lower body temperature in AgRPΔCRFR1 mice (Figure 5C). In addition, hypothalamic expression of *Pomc* and *Mc4r* were found to be lower in AgRPΔCRFR1 mice (Figure 5D). This points toward a reduced melanocortinergic tone that is correlated with diminished energy expenditure in both humans and rodents (Huszar et al., 1997). Overall, these findings suggest that under basal conditions, deletion of CRFR1 in AgRP neurons

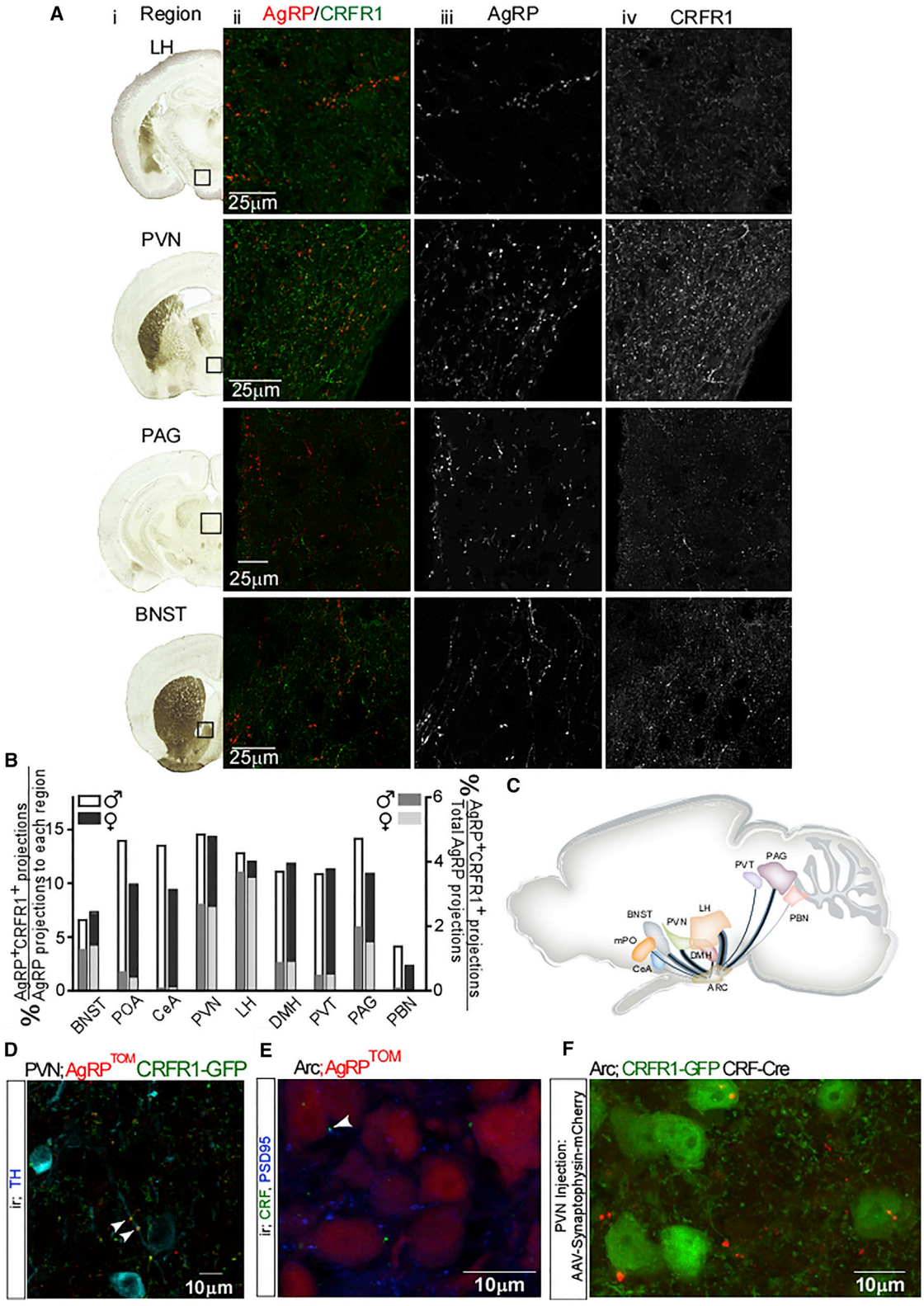

Figure 3. AgRP^{+}CRFR1^{+} Neurons Project Mainly to the LH and PVN and Are Innervated by PVN-CRF Neurons

(A) Nine known AgRP neurons were analyzed for AgRP^{+}CRFR1^{+} projections. (i) Brain coronal section adapted from Paxinos and Franklin's mouse brain atlas (Paxinos and Franklin, 2001). Black box indicates region analyzed. (ii) Overlaid images of AgRP^{TOM} fluorescence and GFP immunoreactivity. (iii) Tomato fluorescence reveals AgRP projections. (iv) GFP immunoreactivity in each region. The scale bar represents 25 μm. See also Figure S2.

(legend continued on next page)

slightly alters energy balance and to some extent mimics AgRP activation as in an energy-deficit state.

Given the role of CRFR1 signaling in integrating the autonomic, metabolic, and behavioral responses to stressors (Brown et al., 1982; Sutton et al., 1982) and the inhibitory action of CRF on AgRP^{+}CRFR1^{+} neurons, we examined whether the differences in heat production could be augmented under a challenge. We exposed the mice to a cold temperature that activates the sympathetic nervous system, resulting in the stimulation of β-adrenergic receptors on brown adipocytes and induces activation and expression of mitochondrial uncoupling protein 1 (UCP1). This adaptive thermogenic process involves heat dissipation by BAT and induces browning of white adipose tissue (WAT) (Harms and Seale, 2013). Shortly following exposure to 5°C, body temperature dropped significantly more in AgRPΔCRFR1 mice, and their temperature remained lower throughout the experiment (Figure 5E). BAT gene expression analysis showed that *Ucp1* transcription was induced to a lesser extent in AgRPΔCRFR1 mice (Figure 5F). Reduced *Ucp1* expression was also demonstrated by IHC with UCP1 antibody (Figure 5G), while expression of *Adrb3*, *Pgc1*, *Dio2*, and *Fgf21* were similar (Figure S5D). In addition, examination of inguinal WAT, which is known to undergo browning following cold exposure, revealed that several browning-related genes, including *Ucp1*, *Pgc1*, *Dio2*, and *Cidea*, are strongly induced in control compared with AgRPΔCRFR1 mice (Figure 5H). These data show impairment in autonomic activation necessary for cold-induced thermogenesis in AgRPΔCRFR1 mice. They further suggest that CRFR1 inhibitory action in AgRP neurons is required for allowing appropriate cold-induced thermogenesis. Interestingly, the described differences were not observed in males. Although *Pomc* mRNA levels were mildly but significantly lower in male AgRPΔCRFR1 mice, they had similar food intake, heat production, body temperature, and response to cold stress as controls (Figures S6A–S6F).

CRFR1 in AgRP Neurons Regulates Hepatic Glucose Production during Fasting

Since AgRP neurons are activated by fasting and have a role in regulating hepatic glucose production (HGP) (Könner et al., 2007), we checked whether the absence of CRFR1 from AgRP neurons affects various functions under fasting. First, we challenged the mice with food deprivation while in the metabolic cages. Soon after fast initiation, AgRPΔCRFR1 mice showed a quicker drop of respiratory exchange ratio (RER) than controls, but once refed, they had a similar rebound RER (Figure 6A). This indicates that upon fasting, AgRPΔCRFR1 mice have an earlier transit from carbohydrates to fatty acids as an energy source, meaning that CRFR1 action in AgRP neurons is required for a balanced transition to fat oxidation. Interestingly, this alteration in energy partitioning during fasting is similar to the one observed in mice lacking Foxo1 in AgRP neurons (Ren et al., 2012).

To check if fat oxidation was preferred because of a reduction in HGP, the hepatic capacity to produce glucose was assessed by a pyruvate challenge after an overnight fast. As suspected, AgRPΔCRFR1 mice had a significantly lower increase in glucose levels (Figure 6B), showing that their adaptation to fasting was probably due to reduced hepatic ability to produce glucose. To study possible mechanisms of decreased gluconeogenesis, we measured hepatic gene expression under basal and fasting state. Although *G6pc* and *Pgc1* expression levels were similar at basal state, fasting induced their expression to a lower extent in AgRPΔCRFR1 mice (Figures 6C and 6D). *Pck* expression was generally lower in AgRPΔCRFR1 mice (main genotype effect) but was not statistically different in the fed or fasted state (Figure 6E), whereas hepatic expression of *Foxo1* and *Fgf21* was similar at basal level and were similarly induced by fasting (Figures S5E and S5F). Interestingly, hypothalamic *Crf* is upregulated during fasting in both genotypes, and corticosterone levels were similarly elevated in the fasting state (Figures 6F and S5G), further supporting the relevance of the CRF circuit under these conditions. The altered kinetics of the RER as well as the differences in HGP observed using pyruvate tolerance test were not observed in male AgRPΔCRFR1 mice (Figures S6G and S6H). Taken together, these data suggest that CRFR1 inhibitory action in AgRP neurons is required for appropriate energy partitioning and maintenance of blood glucose levels during periods of limited energy resources.

DISCUSSION

Classification of Arc-CRFR1-Expressing Neurons

In this work, we have classified the previously uncharacterized population of Arc-CRFR1-expressing neurons. We have found that CRFR1 in this nucleus is composed of several inhibitory subpopulations (AgRP, RIP, and SST neurons). This implies a role for CRFR1 in regulating both energy balance and growth under stressful circumstances in order to promote survival (Figure 6G).

At first, it appeared that a smaller portion of CRFR1 neurons colocalizes with anorexigenic POMC-expressing neurons (using POMC-Cre mice; Figure 1C). However, a deeper examination revealed that the colocalization is only with embryonically labeled POMC neurons that adopt a non-POMC fate during development. It was elegantly shown a few years ago that about a quarter of AgRP neurons arise from POMC progenitors (Padilla et al., 2010). We were able to show that most of POMC-Cre^{+} CRFR1^{+} neurons are AgRP-expressing neurons and therefore suggest that AgRP-CRFR1 neurons can be defined by their embryonic origin, half of which originate from an anorexigenic progenitor marked by POMC-cre. This expression pattern is

(B) Summary of the relative proportion projecting to each region out of AgRP projections and from total AgRP projections to these nine regions.
(C) Schematic diagram of prominent AgRP^{+}CRFR1^{+} neuron axonal projections analyzed in this study. Blue trajectories widths represent the relative AgRP axonal projection to the region. The proportion of AgRP^{+}CRFR1^{+} neurons projection out of total AgRP projection is represented by the black lines.
(D) Immunodetection of PVN-TH neurons in *CRFR1-GFP-AgRP*^{TOM} mice. Arrowheads indicate synaptic contact with AgRP^{+}CRFR1^{+} neurons.
(E) Immunodetection of CRF and PSD95 in the Arc of *AgRP*^{TOM} mice. The arrowhead indicates synaptic contact with CRF neuron.
(F) Immunodetection of GFP in the Arc of *CRFR1-GFP* mice crossed with *CRF-Cre* mice (*CRFR1-GFP-CRF-Cre)* following PVN injection of Cre-dependent mCherry reporter fused to synaptophysin.

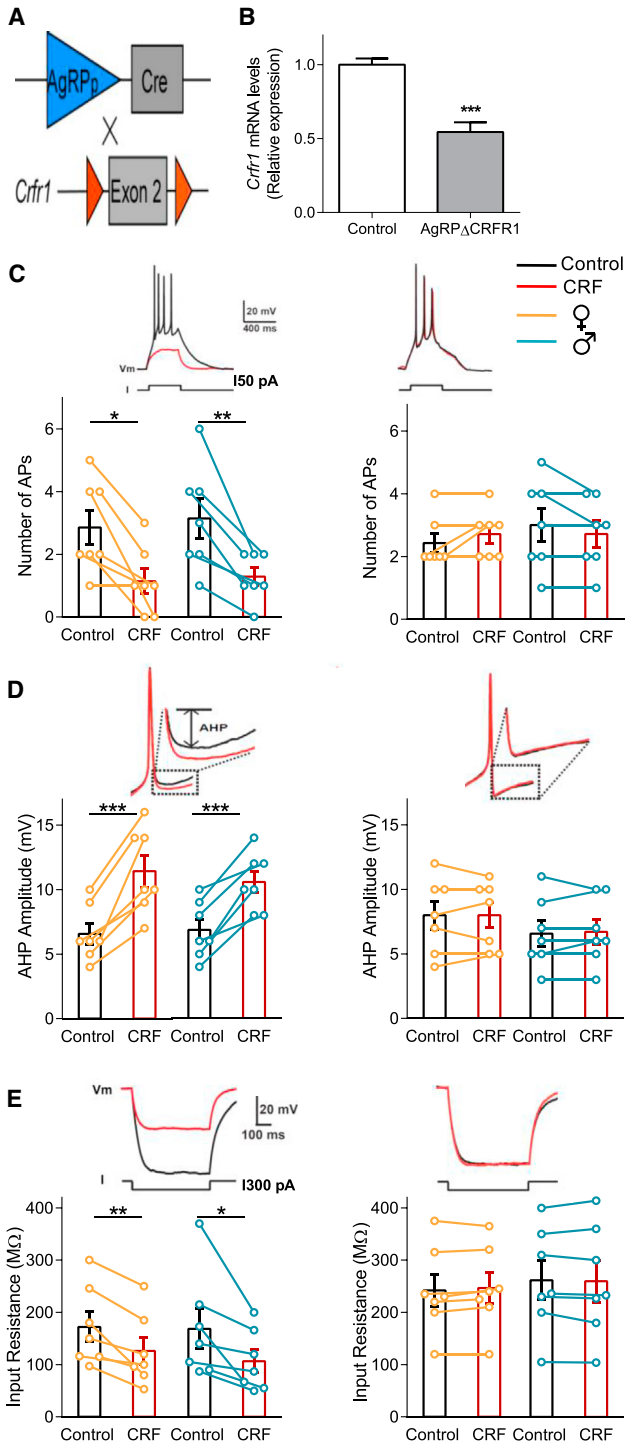

Figure 4. CRFR1-Dependent Reduction of the Excitability of AgRP Neurons

(A) Schematic description of generation of mice lacking CRFR1 in AgRP neurons.

(B) CRFR1 expression level in the MBH of AgRPΔCRFR1 mice and their control littermates.

(C) CRF's effects on firing rate of AgRP$^+$CRFR1$^+$ and AgRPΔCRFR1 neurons. Left: control mice; right: AgRPΔCRFR1 mice. Top: representative recording traces. Orange and blue circles (bottom) depict individual experiments performed in female and male mice, respectively.

(D) CRF's effects on AHP amplitude in AgRP$^+$CRFR1$^+$ and AgRPΔCRFR1 neurons.

(E) CRF's effects on the R_{in} of AgRP$^+$CRFR1$^+$ and AgRPΔCRFR1 neurons.

Control, n = 7 from each sex; AgRPΔCRFR1, n = 7 from each sex. *p < 0.05; **p < 0.01; ***p < 0.001.

supported by a recent study that found that *Crfr1* expression is largely enriched in AgRP compared with POMC isolated neurons (Henry et al., 2015). It is exciting to think that prenatal stressful events may influence the proportion of POMC differentiation through CRFR1. However, the sequentially of embryonic expression suggests that this is not the case. The differentiation of POMC to AgRP occurs at embryonic day (ED) 14.5 (Padilla et al., 2010). Although hypothalamic CRF is already expressed at ED 13.5 (Keegan et al., 1994), CRFR1 expression is observed only at later gestational stages and was shown at ED 17 in rats (Insel et al., 1988) and by ED 18 but not by ED 15 in mice (Allen Brain Atlas), signifying the importance of this circuit for postnatal stages.

Connectivity Mapping of AgRP-CRFR1-Expressing Neurons

Given the vital role of AgRP neurons in controlling hunger, and their exclusive expression pattern, their connectivity was extensively studied (Atasoy et al., 2012; Betley et al., 2013; Dietrich et al., 2012; Krashes et al., 2014). Interestingly, although CRFR1 marks half of AgRP neurons, we found AgRP$^+$CRFR1$^+$ projections in all the inspected terminal fields. The highest proportion of AgRP$^+$CRFR1$^+$/AgRP projections was found in the PVN and the LH, two regions which receive the densest AgRP projections and that were shown to be sufficient for initiating a feeding response by optogenetic stimuli (Betley et al., 2013). Relatively intense projections were found in the BNST, an area implicated in integrating and processing responses to stressful challenges (Sparta et al., 2013). Interestingly, we observed AgRP-CRFR1 fibers in the fusiform and parastrial parts of the BNST, regions that were demonstrated to project to the GABAergic neurons in the LH to evoke feeding (Jennings et al., 2013). Given the PVN's role in regulating food intake and autonomic outflow, its reciprocal connections with AgRP neurons are of special interest. AgRP neurons receive rich inhibitory and excitatory synaptic input, where 70% of the excitatory inputs originate within the hypothalamus, mainly from the PVN, DMH, and VMH (Wang et al., 2015). Excitatory input was shown to affect both basal and fasting-induced feeding (Liu et al., 2012). PVN originating glutamatergic input arises from thyrotropin-releasing hormone- and pituitary adenylate cyclase-activating polypeptide-expressing neurons (Krashes et al., 2014). Here we add the observation that AgRP neurons are also innervated by CRF neurons, suggesting that various stressors may affect the AgRP$^+$CRFR1$^+$ pathway.

Role of CRF Signaling in AgRP Neurons

The storing promoting signal transmitted by AgRP neurons conflicts with immediate catabolic requirements needed during stress. In this light, the inhibitory action of CRF on AgRP$^+$CRFR1$^+$ neurons is perhaps not surprising. However, this inhibitory action is exceptional in the CRF field, as it differs from well-known CRF excitatory effects observed in different brain regions (Aldenhoff

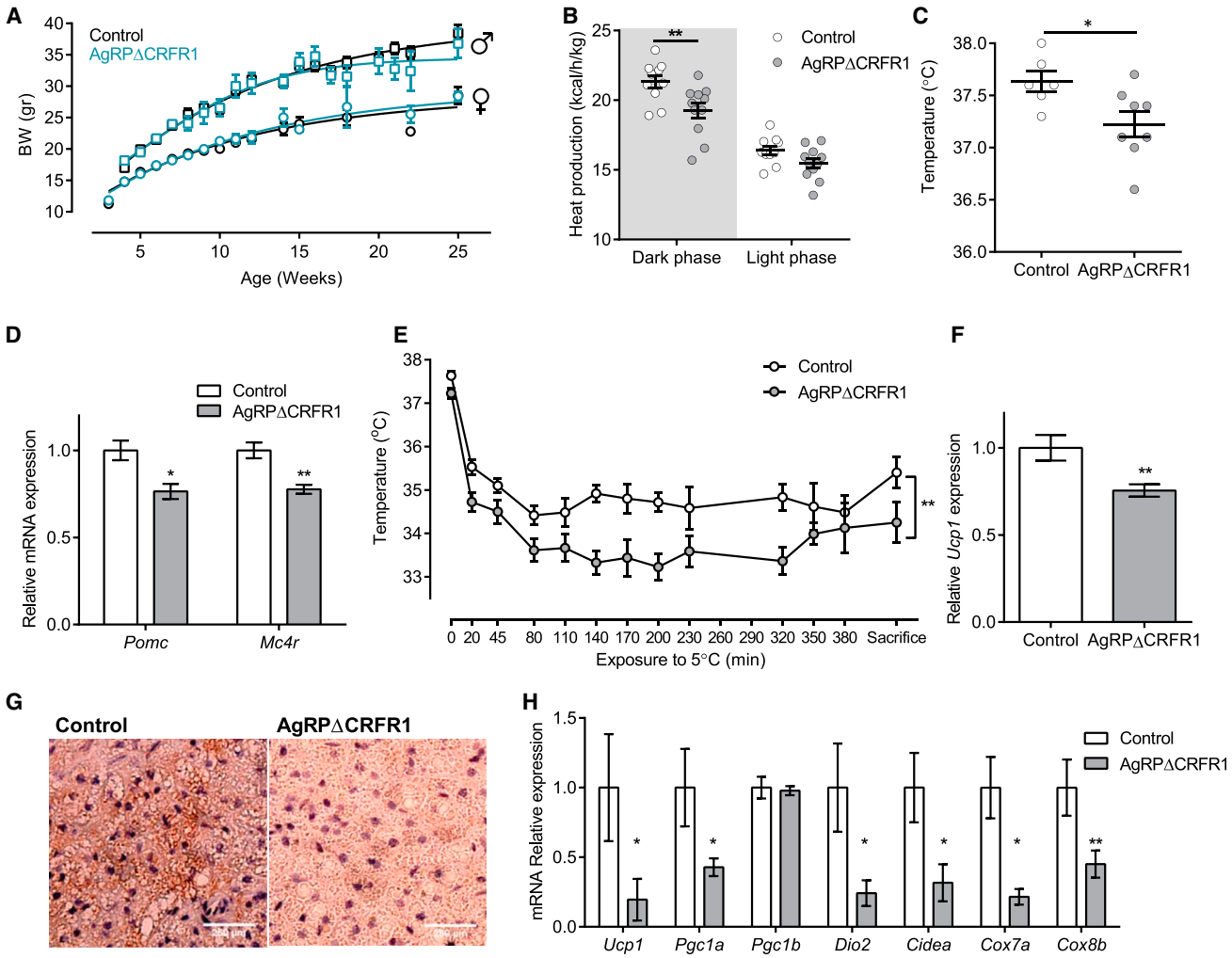

Figure 5. CRFR1 in AgRP Neurons Are Required for Adaptive Thermogenesis

(A) Growth curves of female and male AgRPΔCRFR1 mice and control littermates (n = 3–18).

(B) Heat production of female AgRPΔCRFR1 mice and control littermates (n = 10 and 11).

(C) Body temperature of female AgRPΔCRFR1 mice and control littermates (n = 6 and 8).

(D) Relative *Pomc* and *Mc4r* levels in hypothalami of female AgRPΔCRFR1 mice and control littermates (n = 8–12).

(E) Body temperature during cold challenge test (n = 6 and 8).

(F and G) Relative BAT *Ucp1* expression (F) (n = 6 and 7) and BAT UCP1 immunoreactivity (G) following 7 h at 5°C.

(H) Relative expression of thermogenic-related genes in inguinal WAT following 7 h at 5°C (n = 5–8).

Data are shown as mean ± SEM. *p < 0.05; **p < 0.01. See also Figure S6.

et al., 1983) such as the locus coeruleus (Valentino et al., 1983), the dorsal raphe (Lowry et al., 2000), hypothalamic orexin neurons (Winsky-Sommerer et al., 2004), and the ventral tegmental area (VTA) (Wanat et al., 2008). To date, only one study has reported a similar inhibitory effect of CRF. In that instance, CRF decreased the R_{in} of neurons in the CeA (Rainnie et al., 1992). Interestingly, a recent study showed that optogenetic activation of PVN-CRF neurons failed to evoke excitatory post-synaptic potentials in AgRP neurons (Krashes et al., 2014), ruling out a functional innervation of AgRP neurons by glutamatergic PVN-CRF neurons. The differences between this and our findings may be reconciled by the neuromodulating nature of CRF, which changes the excitability of neurons but does not directly activate ionotropic receptors.

Our electrophysiological results further expand the repertoire of CRF effects showing that CRF decreases AgRP neurons' excitability by increasing the amplitude of the AHP. This effect resembles that of AgRP neurons lacking O-GlcNAc transferase (OGT), where AgRP neuronal excitability was inhibited through modulation of voltage-dependent potassium channels (Ruan et al., 2014).

Given the inhibitory effect of CRF on AgRP neurons, we speculated that the absence of CRF receptors in these neurons would mimic an over-activated state that could alter energy homeostasis because of increased intake or reduced energy expenditure.

With regard to food intake, it is important to note that although AgRP neurons are both mandatory and sufficient for feeding (Aponte et al., 2011; Luquet et al., 2005), several transgenic

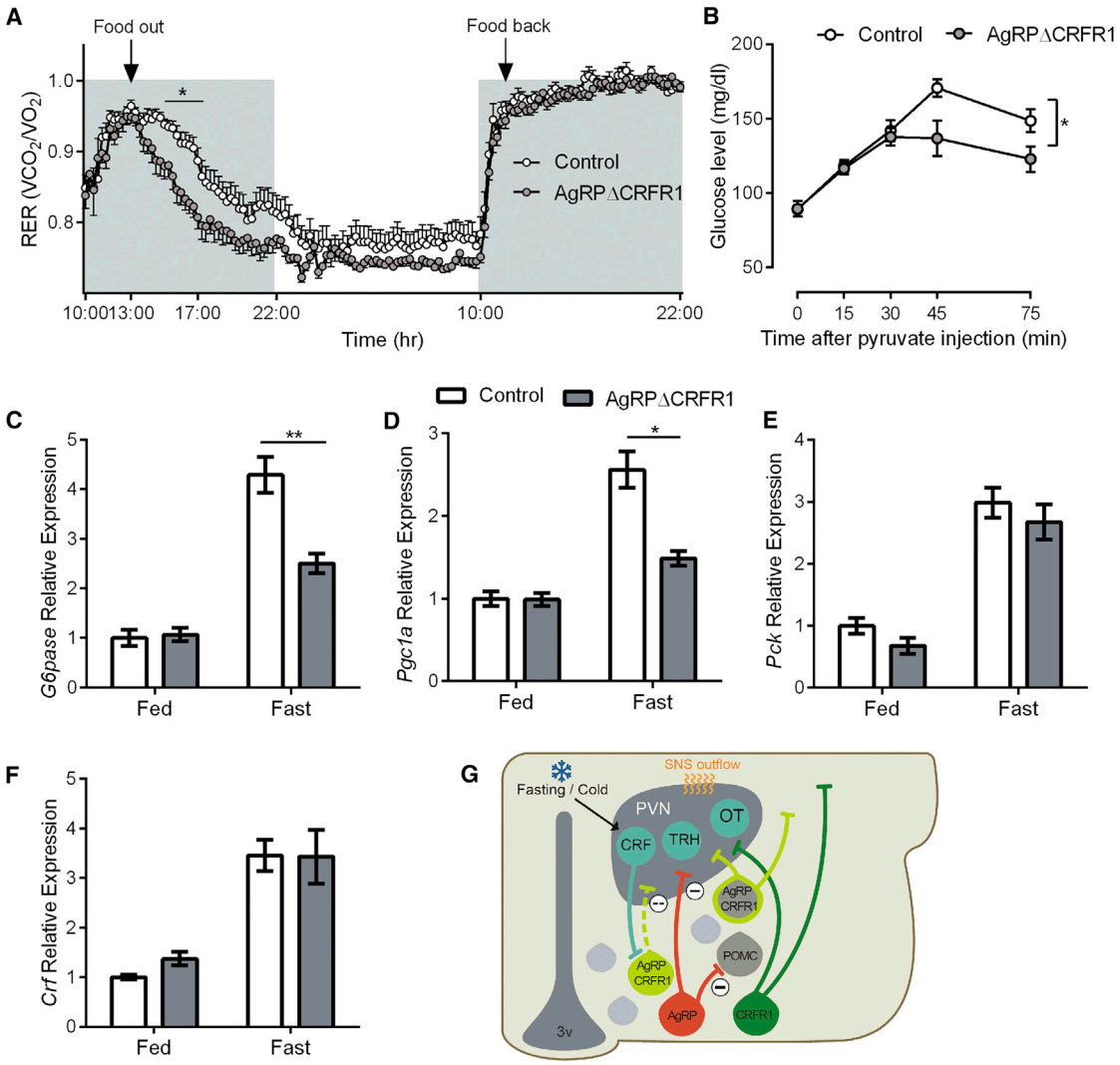

Figure 6. Females' Adaptive Response to Fasting Requires CRFR1 in AgRP Neurons

(A) RER measured during fasting and refeeding in AgRPΔCRFR1 female mice and control littermates (n = 11 and 12).

(B) Glucose levels following a pyruvate challenge (2 g/kg; n = 9–12 females).

(C–F) Relative hepatic expression of *G6pase* (C), *Pgc1a* (D), and *Pck* (E) (n = 6 or 7 females) and hypothalamic expression of *Crf* (F) (n = 7–11 females) at basal state and following 16 hr fast.

(G) In the Arc, half of CRFR1 neurons colocalize with AgRP neurons. About half of these neurons developed from a POMC progenitor. These neurons are activated in fasting or cold conditions by CRF neurons. CRFR1 signaling modulates ion channel activity, leading to hyperpolarization and contributing to increased thermogenesis and HGP under cold or fasting conditions, respectively.

Data are shown as mean ± SEM. *p < 0.05; **p < 0.01.

mice with alterations in key components of the melanocortin system displayed similar food intake. For example, energy homeostasis was altered in neither POMC- nor AgRP-specific insulin receptor KO mice (Könner et al., 2007). Similarly, ablation of leptin receptor from POMC neurons did not alter energy intake (Balthasar et al., 2004; Shi et al., 2008). Additionally, overexpression of constitutive activated STAT3 in AgRP neurons led to leanness, but not as a result of decreased food intake (Mesaros et al., 2008). Also in the present study, the absence of an inhibitory action on AgRP neurons did not affect the consummatory behavior of the mice. This could be attributed to the regulatory nature of the CRF system with effects not necessarily reflected under basal conditions. Furthermore, deletion of CRFR1 occurs in part of AgRP neurons and thus its effects may be masked by the unmanipulated AgRP neuronal population.

Nevertheless, as expected, females lacking CRFR1 in AgRP neurons exhibited a small but significant reduction in heat production. This resembles mice lacking leptin receptor in AgRP neurons, which had lower body temperature with unaltered food intake (van de Wall et al., 2008). The unaltered body weight in light of reduced heat production is puzzling and in the long term is probably balanced by increased physical activity or altered food intake, which was not captured during the measurement window in the metabolic cages.

The anabolic role of AgRP/NPY neurons goes beyond food intake, as was effectively shown by hyperinsulinemia and adiposity in paired fed NPY administered animals (Zarjevski et al., 1993). The inhibitory effect NPY neurons pose on BAT thermogenesis was demonstrated pharmacologically more than 20 years ago by central (Billington et al., 1991) or PVN-NPY administration (Billington et al., 1994). Consistent with this, mice in which NPY is expressed only in the Arc have reduced energy expenditure with lower BAT temperature mediated by reduced expression of PVN-tyrosine hydroxylase (TH) (Shi et al., 2013). The higher sensitivity of mice lacking CRFR1 in AgRP neurons to a cold environment and the reduced induction of browning-related genes in the inguinal WAT supports the idea of mimicking activated AgRP neurons. This is in line with studies showing that AgRP administration decreases BAT temperature (Brito et al., 2007) and that AgRP neuronal activation leads to reduced browning of WAT (Ruan et al., 2014).

It was suggested that under cold conditions, FGF21, acting through β-Klotho in the SCN, stimulates PVN-CRF neurons to induce sympathetic activation (Owen et al., 2014). FGF21 plays a critical role in BAT thermogenesis and in the recruitment of brown-like adipocytes in WAT (Fisher et al., 2012). Our results may be incorporated and add the CRF action on $AgRP^{+}CRFR1^{+}$ neurons, which concurrently reduces AgRP-derived inhibitory tone to allow appropriate sympathetic activation.

Remarkably, we revealed a role of CRFR1 in AgRP neurons in regulating fasting glucose levels by influencing HGP. Endogenous glucose production, primarily by the liver, is an important mechanism for maintaining fasting serum glucose levels (Saltiel, 2001). The PVN plays a key regulatory role in HGP induced by sympathetic activation. Triiodothyronine administration to the PVN increased HGP via sympathetic projections to the liver, independently of circulating glucoregulatory hormones (Klieverik et al., 2009). Furthermore, activation of NMDA receptors or blockade of GABA receptors in the PVN induces HGP due primarily to activation of the sympathetic input to the liver. This induction was shown to depend on removal of GABAergic input to the PVN (Kalsbeek et al., 2004). The GABAergic input was suggested to originate from the SCN. Here we suggest that AgRP neurons contribute further to this phenomenon by delivering GABAergic input to sympathetic preautonomic neurons in the PVN, resulting in an increased HGP. This effect of Arc-CRFR1 is complementary to the counter-regulatory enhancing effect described for VMH-CRFR1 during acute hypoglycemia (Cheng et al., 2007). Overall, activation of the CRFR1 system acts through several mechanisms in different hypothalamic nuclei and aims to defend blood glucose levels.

Interestingly, although the CRF action on electrophysiological properties of $AgRP^{+}CRFR1^{+}$ neurons was similar in males and females, the main differences we found between AgRPΔCRFR1 and control mice were observed only in females. The Arc and AgRP neurons in particular were not associated previously with sexual dimorphism. However, several studies specifically manipulating AgRP neurons provided results obtained from conditional female mice only. For example, ablation of AgRP-VTA pathway increased the development of drug-associated preference in females (Dietrich et al., 2012). Similarly, O-GlcNAc signaling in AgRP neurons was shown to be required for the regulation of WAT browning by fasting and ghrelin, but only results from female mice lacking OGT in AgRP neurons were presented (Ruan et al., 2014). Interestingly, a sex-specific phenotype was observed in females lacking leptin receptor in POMC neurons, which, as in AgRPΔCRFR1 mice, exhibited reduced heat production with unaltered food intake (Shi et al., 2008). Likewise, females lacking STAT3 from POMC neurons have a stronger phenotype with a larger reduction in *Pomc* expression (Xu et al., 2007). These phenotypes could also stem from POMC-originated AgRP neurons that were manipulated (i.e., the same neurons we manipulated in this study). Moreover, in the present study, the sex-specific phenotype could also be attributed to sexual differences in the stress response. Estrogen receptor α is not expressed by AgRP neurons (Olofsson et al., 2009); still, estrogen directly stimulates the CRF promoter and potentiates norepinephrine actions (Vamvakopoulos and Chrousos, 1993, 1994). In this context, it is important to note that within each sex, the differences are independent of HPA function and of GC action, which were unaltered.

Stress-related pathologies might be alleviated by CRFR1 antagonists. Hypoglycemia and reduced thermogenesis, which may lead to obesity, are potential side effects that emerge from the present study because of blockage of Arc-CRFR1. The capacity to block Arc-CRFR1 should also be examined for compounds designed to antagonize peripheral CRF action because of the close proximity to the median eminence lacking an intact blood-brain barrier. This should be considered particularly in women.

From an evolutionary point of view, an organism should have a stronger signal favoring food consumption than satiation in order to survive times with limited access to food. This notion is supported by the observation that a portion of AgRP neurons evolved from neurons with an opposite action. The higher proportion of orexigenic neurons requires governing mechanisms to ensure that other needs will be fulfilled as well. CRFR1 presence in a subpopulation of AgRP neurons provides the organism with such a regulatory tool, acting as a gatekeeper, which assists the organism in recruiting its resources for survival purposes.

EXPERIMENTAL PROCEDURES

Animal Care

Mice were housed and handled in a pathogen-free, temperature-controlled (22°C ± 1°C) mouse facility on a reverse 12/12 hr light/dark cycle, with lights switched on at 10 p.m. The Institutional Animal Care and Use Committee of The Weizmann Institute of Science approved all procedures. Animals were fed a regular chow diet (2018 Teklad Global 18% Protein Rodent Diet). Animals were given ad libitum access to food and water. Food was withdrawn only if required for an experiment.

Immunohistological Analysis

Animals were anesthetized and transcardially perfused with 4% paraformaldehyde (PFA). Brains were post-fixated with 30% sucrose solution in 4% PFA. Fixed brains were serially sectioned (30 μm) and divided into three sets. For quantification, at least two mice were used, and from each mouse a complete set was immunostained and analyzed. Briefly, sections were incubated in blocking solution (20% horse serum, 0.3% Triton in PBS) for 1 hr to prevent nonspecific binding of the antibody. Next, sections were incubated overnight at room temperature with the primary antibody in PBS containing 2% horse serum and 0.3% Triton. Following PBS washes, sections were incubated for

1 hr at room temperature with the appropriate secondary antibodies (Jackson Immunoresearch Laboratories). Sections were washed with PBS and then mounted on slides.

The following antibodies were used: GFP, PSD95, and mCherry (1:250, 1:500, and 1:1,000, respectively; Abcam); ACTH (1:1,000; DAKO); AgRP (1:200; Phoenix Pharmaceuticals); Tyrosin Hydroxylase (1:1,000; Millipore); CRF and SST (both 1:1,000; kindly provided by the late Professor Wylie Vale); pSTAT3 (1:250; Cell Signaling Technology); and c-*fos* (1:1,000; Santa Cruz Biotechnology).

The M.O.M. staining kit (Vector Laboratories) was used when the primary antibody was of mouse origin.

Immunohistochemical staining for UCP1 on BAT was carried out using paraffin sections with the avidin-biotin-peroxidase (avidin biotin complex method; Vector Laboratories) using the rabbit anti-Ucp1 Ab (Abcam). Sections were lightly counterstained with hematoxylin.

Image Analysis

Images were captured using a confocal microscope (Zeiss LSM510 and LSM700). For quantification of AgRP-CRFR1 colocalization, and for assessing pSTAT3, a complete set from each mouse was imaged at 2 μm intervals. For the projections analysis, images were captured at 63× magnification in Z sections of 1 μm intervals. For each terminal field two to six images were analyzed from at least two males and two females. A researcher blind to the slice origin performed quantification of the projections as well as of leptin-responsive neurons using IMMARIS software.

Metabolic Studies

Indirect calorimetry, food and water intake, and locomotor activity were measured using the Labmaster system (TSE-Systems), as previously described (Kuperman et al., 2010). Food deprivation was initiated 3 hr after the beginning of the dark phase, and the refeeding period started at the beginning of the subsequent dark phase.

Body Temperature Measurements

Mice were implanted with an Implantable Programmable Temperature and Identification Transponder (IPTT-300; Bio Medic Data Systems) under isoflurane anesthesia. Body temperature data were obtained using a SP-6005 reader (Bio Medic Data Systems).

Statistical Analyses

Values are expressed as mean ± SEM. Statistical analysis was performed using repeated-measures two-way ANOVA with Bonferroni post hoc t tests or Student's t tests as appropriate, using Prism software (GraphPad Software).

SUPPLEMENTAL INFORMATION

Supplemental Information includes Supplemental Experimental Procedures and six figures and can be found with this article online at http://dx.doi.org/10.1016/j.cmet.2016.04.017.

AUTHOR CONTRIBUTIONS

Y.K. and M.W. designed and performed most of the experiments. J.D., M.E., W.W., and J.M.D. designed and performed electrophysiological studies. K.S., A.R., T.N., C.K., and Y.S. assisted in experiments. O.G. wrote the code for analyzing the projection fields. Y.K., M.W., A.H., and A.C. conceived, designed, and supervised the project. Y.K. and A.C. wrote the manuscript.

ACKNOWLEDGMENTS

A.C. is head of the Max Planck Society, Weizmann Institute of Science Laboratory for Experimental Neuropsychiatry and Behavioral Neurogenetics. Y.K. is the incumbent of the Sarah and Rolando Uziel Research Associate Chair. We thank Mr. Sharon Ovadia and Ms. Dalia Vaknin for their devoted assistance with animal care. We thank Dr. Jessica Keverne for professional English editing, formatting, and scientific input. This work is supported by an FP7 grant from the European Research Council (260463); research support from the Perlman Family Foundation, founded by Louis L. and Anita M. Perlman; a research grant from the Israel Science Foundation (803/11); research support from Roberto and Renata Ruhman; the Nella and Leon Benoziyo Center for Neurological Diseases; the Henry Chanoch Krenter Institute for Biomedical Imaging and Genomics; the Adelis Foundation; the Irving I. Moskowitz Foundation; and the Helmholtz Alliance ICEMED, Imaging and Curing Environmental Metabolic Diseases, through the Initiative and Network Fund of the Helmholtz Association (to J.M.D. and W.W.).

We dedicate this work to the memory of Professor W. Vale (Salk Institute for Biological Studies).

Received: October 5, 2015
Revised: February 12, 2016
Accepted: April 22, 2016
Published: May 19, 2016

REFERENCES

Aldenhoff, J.B., Gruol, D.L., Rivier, J., Vale, W., and Siggins, G.R. (1983). Corticotropin releasing factor decreases postburst hyperpolarizations and excites hippocampal neurons. Science *221*, 875–877.

Aponte, Y., Atasoy, D., and Sternson, S.M. (2011). AGRP neurons are sufficient to orchestrate feeding behavior rapidly and without training. Nat. Neurosci. *14*, 351–355.

Arase, K., York, D.A., Shimizu, H., Shargill, N., and Bray, G.A. (1988). Effects of corticotropin-releasing factor on food intake and brown adipose tissue thermogenesis in rats. Am. J. Physiol. *255*, E255–E259.

Atasoy, D., Betley, J.N., Su, H.H., and Sternson, S.M. (2012). Deconstruction of a neural circuit for hunger. Nature *488*, 172–177.

Balthasar, N., Coppari, R., McMinn, J., Liu, S.M., Lee, C.E., Tang, V., Kenny, C.D., McGovern, R.A., Chua, S.C., Jr., Elmquist, J.K., and Lowell, B.B. (2004). Leptin receptor signaling in POMC neurons is required for normal body weight homeostasis. Neuron *42*, 983–991.

Bamshad, M., Song, C.K., and Bartness, T.J. (1999). CNS origins of the sympathetic nervous system outflow to brown adipose tissue. Am. J. Physiol. *276*, R1569–R1578.

Betley, J.N., Cao, Z.F., Ritola, K.D., and Sternson, S.M. (2013). Parallel, redundant circuit organization for homeostatic control of feeding behavior. Cell *155*, 1337–1350.

Billington, C.J., Briggs, J.E., Grace, M., and Levine, A.S. (1991). Effects of intracerebroventricular injection of neuropeptide Y on energy metabolism. Am. J. Physiol. *260*, R321–R327.

Billington, C.J., Briggs, J.E., Harker, S., Grace, M., and Levine, A.S. (1994). Neuropeptide Y in hypothalamic paraventricular nucleus: a center coordinating energy metabolism. Am. J. Physiol. *266*, R1765–R1770.

Bluet-Pajot, M.T., Epelbaum, J., Gourdji, D., Hammond, C., and Kordon, C. (1998). Hypothalamic and hypophyseal regulation of growth hormone secretion. Cell. Mol. Neurobiol. *18*, 101–123.

Brito, M.N., Brito, N.A., Baro, D.J., Song, C.K., and Bartness, T.J. (2007). Differential activation of the sympathetic innervation of adipose tissues by melanocortin receptor stimulation. Endocrinology *148*, 5339–5347.

Broberger, C., Johansen, J., Johansson, C., Schalling, M., and Hökfelt, T. (1998). The neuropeptide Y/agouti gene-related protein (AGRP) brain circuitry in normal, anorectic, and monosodium glutamate-treated mice. Proc. Natl. Acad. Sci. U S A *95*, 15043–15048.

Brown, M.R., Fisher, L.A., Spiess, J., Rivier, C., Rivier, J., and Vale, W. (1982). Corticotropin-releasing factor: actions on the sympathetic nervous system and metabolism. Endocrinology *111*, 928–931.

Cerri, M., and Morrison, S.F. (2006). Corticotropin releasing factor increases in brown adipose tissue thermogenesis and heart rate through dorsomedial hypothalamus and medullary raphe pallidus. Neuroscience *140*, 711–721.

Cheng, H., Zhou, L., Zhu, W., Wang, A., Tang, C., Chan, O., Sherwin, R.S., and McCrimmon, R.J. (2007). Type 1 corticotropin-releasing factor receptors in the ventromedial hypothalamus promote hypoglycemia-induced hormonal counterregulation. Am. J. Physiol. Endocrinol. Metab. *293*, E705–E712.

Clegg, D.J., Riedy, C.A., Smith, K.A., Benoit, S.C., and Woods, S.C. (2003). Differential sensitivity to central leptin and insulin in male and female rats. Diabetes *52*, 682–687.

Cole, R.L., and Sawchenko, P.E. (2002). Neurotransmitter regulation of cellular activation and neuropeptide gene expression in the paraventricular nucleus of the hypothalamus. J. Neurosci. *22*, 959–969.

Cone, R.D. (2005). Anatomy and regulation of the central melanocortin system. Nat. Neurosci. *8*, 571–578.

Dietrich, M.O., Bober, J., Ferreira, J.G., Tellez, L.A., Mineur, Y.S., Souza, D.O., Gao, X.B., Picciotto, M.R., Araújo, I., Liu, Z.W., and Horvath, T.L. (2012). AgRP neurons regulate development of dopamine neuronal plasticity and nonfood-associated behaviors. Nat. Neurosci. *15*, 1108–1110.

Fisher, L.A., Rivier, J., Rivier, C., Spiess, J., Vale, W., and Brown, M.R. (1982). Corticotropin-releasing factor (CRF): central effects on mean arterial pressure and heart rate in rats. Endocrinology *110*, 2222–2224.

Fisher, F.M., Kleiner, S., Douris, N., Fox, E.C., Mepani, R.J., Verdeguer, F., Wu, J., Kharitonenkov, A., Flier, J.S., Maratos-Flier, E., and Spiegelman, B.M. (2012). FGF21 regulates PGC-1α and browning of white adipose tissues in adaptive thermogenesis. Genes Dev. *26*, 271–281.

Griebel, G., Simiand, J., Steinberg, R., Jung, M., Gully, D., Roger, P., Geslin, M., Scatton, B., Maffrand, J.P., and Soubrié, P. (2002). 4-(2-Chloro-4-methoxy-5-methylphenyl)-N-[(1S)-2-cyclopropyl-1-(3-fluoro-4-methylphenyl) ethyl]5-methyl-N-(2-propynyl)-1, 3-thiazol-2-amine hydrochloride (SSR125543A), a potent and selective corticotrophin-releasing factor(1) receptor antagonist. II. Characterization in rodent models of stress-related disorders. J. Pharmacol. Exp. Ther. *301*, 333–345.

Harms, M., and Seale, P. (2013). Brown and beige fat: development, function and therapeutic potential. Nat. Med. *19*, 1252–1263.

Henry, F.E., Sugino, K., Tozer, A., Branco, T., and Sternson, S.M. (2015). Cell type-specific transcriptomics of hypothalamic energy-sensing neuron responses to weight-loss. eLife *4*, 4.

Herman, J.P., Ostrander, M.M., Mueller, N.K., and Figueiredo, H. (2005). Limbic system mechanisms of stress regulation: hypothalamo-pituitary-adrenocortical axis. Prog. Neuropsychopharmacol. Biol. Psychiatry *29*, 1201–1213.

Huszar, D., Lynch, C.A., Fairchild-Huntress, V., Dunmore, J.H., Fang, Q., Berkemeier, L.R., Gu, W., Kesterson, R.A., Boston, B.A., Cone, R.D., et al. (1997). Targeted disruption of the melanocortin-4 receptor results in obesity in mice. Cell *88*, 131–141.

Insel, T.R., Battaglia, G., Fairbanks, D.W., and De Souza, E.B. (1988). The ontogeny of brain receptors for corticotropin-releasing factor and the development of their functional association with adenylate cyclase. J. Neurosci. *8*, 4151–4158.

Jennings, J.H., Rizzi, G., Stamatakis, A.M., Ung, R.L., and Stuber, G.D. (2013). The inhibitory circuit architecture of the lateral hypothalamus orchestrates feeding. Science *341*, 1517–1521.

Justice, N.J., Yuan, Z.F., Sawchenko, P.E., and Vale, W. (2008). Type 1 corticotropin-releasing factor receptor expression reported in BAC transgenic mice: implications for reconciling ligand-receptor mismatch in the central corticotropin-releasing factor system. J. Comp. Neurol. *511*, 479–496.

Kalsbeek, A., La Fleur, S., Van Heijningen, C., and Buijs, R.M. (2004). Suprachiasmatic GABAergic inputs to the paraventricular nucleus control plasma glucose concentrations in the rat via sympathetic innervation of the liver. J. Neurosci. *24*, 7604–7613.

Kannan, H., Hayashida, Y., and Yamashita, H. (1989). Increase in sympathetic outflow by paraventricular nucleus stimulation in awake rats. Am. J. Physiol. *256*, R1325–R1330.

Keegan, C.E., Herman, J.P., Karolyi, I.J., O'Shea, K.S., Camper, S.A., and Seasholtz, A.F. (1994). Differential expression of corticotropin-releasing hormone in developing mouse embryos and adult brain. Endocrinology *134*, 2547–2555.

Klieverik, L.P., Janssen, S.F., van Riel, A., Foppen, E., Bisschop, P.H., Serlie, M.J., Boelen, A., Ackermans, M.T., Sauerwein, H.P., Fliers, E., and Kalsbeek, A. (2009). Thyroid hormone modulates glucose production via a sympathetic pathway from the hypothalamic paraventricular nucleus to the liver. Proc. Natl. Acad. Sci. U S A *106*, 5966–5971.

Kong, D., Tong, Q., Ye, C., Koda, S., Fuller, P.M., Krashes, M.J., Vong, L., Ray, R.S., Olson, D.P., and Lowell, B.B. (2012). GABAergic RIP-Cre neurons in the arcuate nucleus selectively regulate energy expenditure. Cell *151*, 645–657.

Könner, A.C., Janoschek, R., Plum, L., Jordan, S.D., Rother, E., Ma, X., Xu, C., Enriori, P., Hampel, B., Barsh, G.S., et al. (2007). Insulin action in AgRP-expressing neurons is required for suppression of hepatic glucose production. Cell Metab. *5*, 438–449.

Krashes, M.J., Shah, B.P., Madara, J.C., Olson, D.P., Strochlic, D.E., Garfield, A.S., Vong, L., Pei, H., Watabe-Uchida, M., Uchida, N., et al. (2014). An excitatory paraventricular nucleus to AgRP neuron circuit that drives hunger. Nature *507*, 238–242.

Kuperman, Y., Issler, O., Regev, L., Musseri, I., Navon, I., Neufeld-Cohen, A., Gil, S., and Chen, A. (2010). Perifornical Urocortin-3 mediates the link between stress-induced anxiety and energy homeostasis. Proc. Natl. Acad. Sci. U S A *107*, 8393–8398.

la Fleur, S.E., Kalsbeek, A., Wortel, J., and Buijs, R.M. (2000). Polysynaptic neural pathways between the hypothalamus, including the suprachiasmatic nucleus, and the liver. Brain Res. *871*, 50–56.

LeFeuvre, R.A., Rothwell, N.J., and Stock, M.J. (1987). Activation of brown fat thermogenesis in response to central injection of corticotropin releasing hormone in the rat. Neuropharmacology *26*, 1217–1221.

Lehman, M.N., Hileman, S.M., and Goodman, R.L. (2013). Neuroanatomy of the kisspeptin signaling system in mammals: comparative and developmental aspects. Adv. Exp. Med. Biol. *784*, 27–62.

Lewis, K., Li, C., Perrin, M.H., Blount, A., Kunitake, K., Donaldson, C., Vaughan, J., Reyes, T.M., Gulyas, J., Fischer, W., et al. (2001). Identification of urocortin III, an additional member of the corticotropin-releasing factor (CRF) family with high affinity for the CRF2 receptor. Proc. Natl. Acad. Sci. U S A *98*, 7570–7575.

Liu, T., Kong, D., Shah, B.P., Ye, C., Koda, S., Saunders, A., Ding, J.B., Yang, Z., Sabatini, B.L., and Lowell, B.B. (2012). Fasting activation of AgRP neurons requires NMDA receptors and involves spinogenesis and increased excitatory tone. Neuron *73*, 511–522.

Lowry, C.A., Rodda, J.E., Lightman, S.L., and Ingram, C.D. (2000). Corticotropin-releasing factor increases in vitro firing rates of serotonergic neurons in the rat dorsal raphe nucleus: evidence for activation of a topographically organized mesolimbocortical serotonergic system. J. Neurosci. *20*, 7728–7736.

Luquet, S., Perez, F.A., Hnasko, T.S., and Palmiter, R.D. (2005). NPY/AgRP neurons are essential for feeding in adult mice but can be ablated in neonates. Science *310*, 683–685.

Madden, C.J., and Morrison, S.F. (2009). Neurons in the paraventricular nucleus of the hypothalamus inhibit sympathetic outflow to brown adipose tissue. Am. J. Physiol. Regul. Integr. Comp. Physiol. *296*, R831–R843.

Madisen, L., Zwingman, T.A., Sunkin, S.M., Oh, S.W., Zariwala, H.A., Gu, H., Ng, L.L., Palmiter, R.D., Hawrylycz, M.J., Jones, A.R., et al. (2010). A robust and high-throughput Cre reporting and characterization system for the whole mouse brain. Nat. Neurosci. *13*, 133–140.

Mesaros, A., Koralov, S.B., Rother, E., Wunderlich, F.T., Ernst, M.B., Barsh, G.S., Rajewsky, K., and Brüning, J.C. (2008). Activation of Stat3 signaling in AgRP neurons promotes locomotor activity. Cell Metab. *7*, 236–248.

Müller, M.B., Zimmermann, S., Sillaber, I., Hagemeyer, T.P., Deussing, J.M., Timpl, P., Kormann, M.S., Droste, S.K., Kühn, R., Reul, J.M., et al. (2003). Limbic corticotropin-releasing hormone receptor 1 mediates anxiety-related behavior and hormonal adaptation to stress. Nat. Neurosci. *6*, 1100–1107.

Niimi, M., Takahara, J., Hashimoto, K., and Kawanishi, K. (1988). Immunohistochemical identification of corticotropin releasing factor-containing neurons projecting to the stalk-median eminence of the rat. Peptides *9*, 589–593.

Oh, S.W., Harris, J.A., Ng, L., Winslow, B., Cain, N., Mihalas, S., Wang, Q., Lau, C., Kuan, L., Henry, A.M., et al. (2014). A mesoscale connectome of the mouse brain. Nature *508*, 207–214.

Olofsson, L.E., Pierce, A.A., and Xu, A.W. (2009). Functional requirement of AgRP and NPY neurons in ovarian cycle-dependent regulation of food intake. Proc. Natl. Acad. Sci. USA *106*, 15932–15937.

Owen, B.M., Ding, X., Morgan, D.A., Coate, K.C., Bookout, A.L., Rahmouni, K., Kliewer, S.A., and Mangelsdorf, D.J. (2014). FGF21 acts centrally to induce sympathetic nerve activity, energy expenditure, and weight loss. Cell Metab. *20*, 670–677.

Padilla, S.L., Carmody, J.S., and Zeltser, L.M. (2010). Pomc-expressing progenitors give rise to antagonistic neuronal populations in hypothalamic feeding circuits. Nat. Med. *16*, 403–405.

Padilla, S.L., Reef, D., and Zeltser, L.M. (2012). Defining POMC neurons using transgenic reagents: impact of transient Pomc expression in diverse immature neuronal populations. Endocrinology *153*, 1219–1231.

Paxinos, G., and Franklin, K.B.J. (2001). The Mouse Brain in Stereotaxic Coordinates (San Diego: Academic).

Rainnie, D.G., Fernhout, B.J., and Shinnick-Gallagher, P. (1992). Differential actions of corticotropin releasing factor on basolateral and central amygdaloid neurones, in vitro. J. Pharmacol. Exp. Ther. *263*, 846–858.

Refojo, D., Schweizer, M., Kuehne, C., Ehrenberg, S., Thoeringer, C., Vogl, A.M., Dedic, N., Schumacher, M., von Wolff, G., Avrabos, C., et al. (2011). Glutamatergic and dopaminergic neurons mediate anxiogenic and anxiolytic effects of CRHR1. Science *333*, 1903–1907.

Ren, H., Orozco, I.J., Su, Y., Suyama, S., Gutiérrez-Juárez, R., Horvath, T.L., Wardlaw, S.L., Plum, L., Arancio, O., and Accili, D. (2012). FoxO1 target Gpr17 activates AgRP neurons to regulate food intake. Cell *149*, 1314–1326.

Reyes, T.M., Lewis, K., Perrin, M.H., Kunitake, K.S., Vaughan, J., Arias, C.A., Hogenesch, J.B., Gulyas, J., Rivier, J., Vale, W.W., and Sawchenko, P.E. (2001). Urocortin II: a member of the corticotropin-releasing factor (CRF) neuropeptide family that is selectively bound by type 2 CRF receptors. Proc. Natl. Acad. Sci. U S A *98*, 2843–2848.

Roland, B.L., and Sawchenko, P.E. (1993). Local origins of some GABAergic projections to the paraventricular and supraoptic nuclei of the hypothalamus in the rat. J. Comp. Neurol. *332*, 123–143.

Ruan, H.B., Dietrich, M.O., Liu, Z.W., Zimmer, M.R., Li, M.D., Singh, J.P., Zhang, K., Yin, R., Wu, J., Horvath, T.L., and Yang, X. (2014). O-GlcNAc transferase enables AgRP neurons to suppress browning of white fat. Cell *159*, 306–317.

Saltiel, A.R. (2001). New perspectives into the molecular pathogenesis and treatment of type 2 diabetes. Cell *104*, 517–529.

Shi, H., Strader, A.D., Sorrell, J.E., Chambers, J.B., Woods, S.C., and Seeley, R.J. (2008). Sexually different actions of leptin in proopiomelanocortin neurons to regulate glucose homeostasis. Am. J. Physiol. Endocrinol. Metab. *294*, E630–E639.

Shi, Y.C., Lau, J., Lin, Z., Zhang, H., Zhai, L., Sperk, G., Heilbronn, R., Mietzsch, M., Weger, S., Huang, X.F., et al. (2013). Arcuate NPY controls sympathetic output and BAT function via a relay of tyrosine hydroxylase neurons in the PVN. Cell Metab. *17*, 236–248.

Smith, G.W., Aubry, J.M., Dellu, F., Contarino, A., Bilezikjian, L.M., Gold, L.H., Chen, R., Marchuk, Y., Hauser, C., Bentley, C.A., et al. (1998). Corticotropin releasing factor receptor 1-deficient mice display decreased anxiety, impaired stress response, and aberrant neuroendocrine development. Neuron *20*, 1093–1102.

Sparta, D.R., Jennings, J.H., Ung, R.L., and Stuber, G.D. (2013). Optogenetic strategies to investigate neural circuitry engaged by stress. Behav. Brain Res. *255*, 19–25.

Sternson, S.M. (2013). Hypothalamic survival circuits: blueprints for purposive behaviors. Neuron *77*, 810–824.

Sutton, R.E., Koob, G.F., Le Moal, M., Rivier, J., and Vale, W. (1982). Corticotropin releasing factor produces behavioural activation in rats. Nature *297*, 331–333.

Swanson, L.W., and Sawchenko, P.E. (1980). Paraventricular nucleus: a site for the integration of neuroendocrine and autonomic mechanisms. Neuroendocrinology *31*, 410–417.

Swanson, L.W., Sawchenko, P.E., Rivier, J., and Vale, W.W. (1983). Organization of ovine corticotropin-releasing factor immunoreactive cells and fibers in the rat brain: an immunohistochemical study. Neuroendocrinology *36*, 165–186.

Taniguchi, H., He, M., Wu, P., Kim, S., Paik, R., Sugino, K., Kvitsiani, D., Fu, Y., Lu, J., Lin, Y., et al. (2011). A resource of Cre driver lines for genetic targeting of GABAergic neurons in cerebral cortex. Neuron *71*, 995–1013.

Timpl, P., Spanagel, R., Sillaber, I., Kresse, A., Reul, J.M., Stalla, G.K., Blanquet, V., Steckler, T., Holsboer, F., and Wurst, W. (1998). Impaired stress response and reduced anxiety in mice lacking a functional corticotropin-releasing hormone receptor 1. Nat. Genet. *19*, 162–166.

Tong, Q., Ye, C.P., Jones, J.E., Elmquist, J.K., and Lowell, B.B. (2008). Synaptic release of GABA by AgRP neurons is required for normal regulation of energy balance. Nat. Neurosci. *11*, 998–1000.

Ulrich-Lai, Y.M., and Herman, J.P. (2009). Neural regulation of endocrine and autonomic stress responses. Nat. Rev. Neurosci. *10*, 397–409.

Vale, W., Spiess, J., Rivier, C., and Rivier, J. (1981). Characterization of a 41-residue ovine hypothalamic peptide that stimulates secretion of corticotropin and beta-endorphin. Science *213*, 1394–1397.

Valentino, R.J., Foote, S.L., and Aston-Jones, G. (1983). Corticotropin-releasing factor activates noradrenergic neurons of the locus coeruleus. Brain Res. *270*, 363–367.

Vamvakopoulos, N.C., and Chrousos, G.P. (1993). Evidence of direct estrogenic regulation of human corticotropin-releasing hormone gene expression. Potential implications for the sexual dimophism of the stress response and immune/inflammatory reaction. J. Clin. Invest. *92*, 1896–1902.

Vamvakopoulos, N.C., and Chrousos, G.P. (1994). Hormonal regulation of human corticotropin-releasing hormone gene expression: implications for the stress response and immune/inflammatory reaction. Endocr. Rev. *15*, 409–420.

van de Wall, E., Leshan, R., Xu, A.W., Balthasar, N., Coppari, R., Liu, S.M., Jo, Y.H., MacKenzie, R.G., Allison, D.B., Dun, N.J., et al. (2008). Collective and individual functions of leptin receptor modulated neurons controlling metabolism and ingestion. Endocrinology *149*, 1773–1785.

van den Top, M., Lee, K., Whyment, A.D., Blanks, A.M., and Spanswick, D. (2004). Orexigen-sensitive NPY/AgRP pacemaker neurons in the hypothalamic arcuate nucleus. Nat. Neurosci. *7*, 493–494.

Van Pett, K., Viau, V., Bittencourt, J.C., Chan, R.K., Li, H.Y., Arias, C., Prins, G.S., Perrin, M., Vale, W., and Sawchenko, P.E. (2000). Distribution of mRNAs encoding CRF receptors in brain and pituitary of rat and mouse. J. Comp. Neurol. *428*, 191–212.

Vaughan, J., Donaldson, C., Bittencourt, J., Perrin, M.H., Lewis, K., Sutton, S., Chan, R., Turnbull, A.V., Lovejoy, D., Rivier, C., et al. (1995). Urocortin, a mammalian neuropeptide related to fish urotensin I and to corticotropin-releasing factor. Nature *378*, 287–292.

Viñuela, M.C., and Larsen, P.J. (2001). Identification of NPY-induced c-Fos expression in hypothalamic neurones projecting to the dorsal vagal complex and the lower thoracic spinal cord. J. Comp. Neurol. *438*, 286–299.

Wanat, M.J., Hopf, F.W., Stuber, G.D., Phillips, P.E., and Bonci, A. (2008). Corticotropin-releasing factor increases mouse ventral tegmental area dopamine neuron firing through a protein kinase C-dependent enhancement of Ih. J. Physiol. *586*, 2157–2170.

Wang, L., Saint-Pierre, D.H., and Taché, Y. (2002). Peripheral ghrelin selectively increases Fos expression in neuropeptide Y - synthesizing neurons in mouse hypothalamic arcuate nucleus. Neurosci. Lett. *325*, 47–51.

Wang, D., He, X., Zhao, Z., Feng, Q., Lin, R., Sun, Y., Ding, T., Xu, F., Luo, M., and Zhan, C. (2015). Whole-brain mapping of the direct inputs and axonal projections of POMC and AgRP neurons. Front. Neuroanat. *9*, 40.

Winsky-Sommerer, R., Yamanaka, A., Diano, S., Borok, E., Roberts, A.J., Sakurai, T., Kilduff, T.S., Horvath, T.L., and de Lecea, L. (2004). Interaction between the corticotropin-releasing factor system and hypocretins (orexins): a novel circuit mediating stress response. J. Neurosci. *24*, 11439–11448.

Wu, Q., Boyle, M.P., and Palmiter, R.D. (2009). Loss of GABAergic signaling by AgRP neurons to the parabrachial nucleus leads to starvation. Cell *137*, 1225–1234.

Xu, A.W., Ste-Marie, L., Kaelin, C.B., and Barsh, G.S. (2007). Inactivation of signal transducer and activator of transcription 3 in proopiomelanocortin (Pomc) neurons causes decreased pomc expression, mild obesity, and defects in compensatory refeeding. Endocrinology *148*, 72–80.

Zarjevski, N., Cusin, I., Vettor, R., Rohner-Jeanrenaud, F., and Jeanrenaud, B. (1993). Chronic intracerebroventricular neuropeptide-Y administration to normal rats mimics hormonal and metabolic changes of obesity. Endocrinology *133*, 1753–1758.

Cell Metabolism, Volume *23*

Supplemental Information

CRFR1 in AgRP Neurons Modulates Sympathetic Nervous System Activity to Adapt to Cold Stress and Fasting

Yael Kuperman, Meira Weiss, Julien Dine, Katy Staikin, Ofra Golani, Assaf Ramot, Tali Nahum, Claudia Kühne, Yair Shemesh, Wolfgang Wurst, Alon Harmelin, Jan M. Deussing, Matthias Eder, and Alon Chen

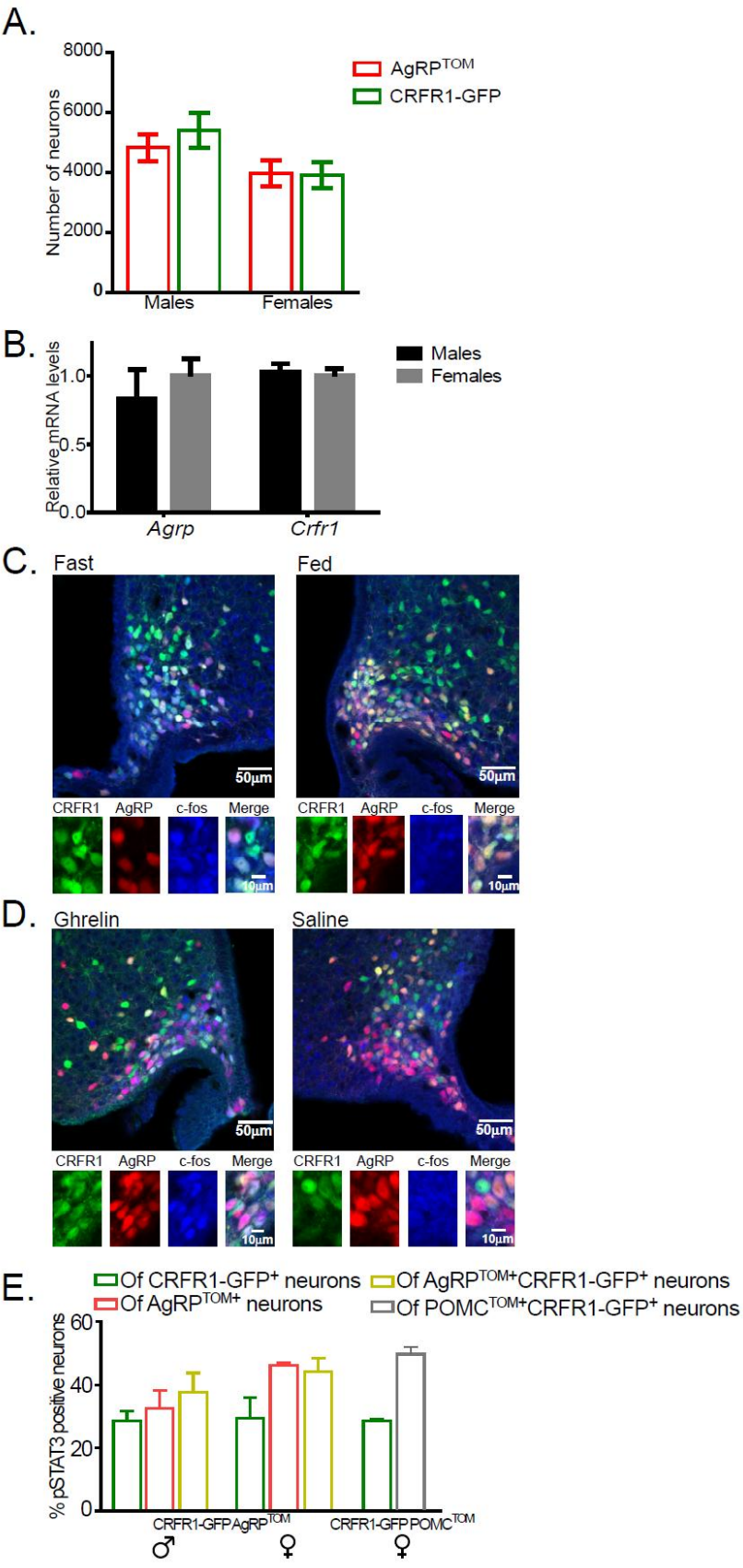
A.
8000
6000
4000
2000
0
Number of neurons
AgRP^TOM
CRFR1-GFP
Males
Females
B.
1.0
0.5
0.0
Relative mRNA levels
Males
Females
Agrp
Crfr1
C.
Fast
Fed
50µm
CRFR1
AgRP
c-fos
Merge
10µm
D.
Ghrelin
Saline
E.
Of CRFR1-GFP+ neurons
Of AgRP^TOM+ neurons
Of AgRP^TOM+CRFR1-GFP+ neurons
Of POMC^TOM+CRFR1-GFP+ neurons
60
40
20
0
% pSTAT3 positive neurons
CRFR1-GFP AgRP^TOM
CRFR1-GFP POMC^TOM
♂
♀
♀

Figure S1. Characterization of AgRP^{+}CRFR1^{+} neurons. Related to Figure 1.

A. Number of CRFR1-GFP and AgRP^{TOM} neurons in males and females *CRFR1-GFP-AGRP^{TOM}* mice (n=7 for each sex).

B. Relative *Crfr1* and *Agrp* expression in the MBH of WT ICR mice (n=9 for each sex).

C. Immunostaining of c-Fos in the Arc of fed and overnight-fasted *CRFR1-GFP-AgRP^{TOM}* reporter mice.

D. Immunostaining of c-Fos in the Arc of ghrelin or saline injected *CRFR1-GFP-AgRP^{TOM}* reporter mice.

E. Percentage of pSTAT3 positive neurons out of CRFR1-GFP^{+}/AgRP^{TOM+}/CRFR1-GFP-AgRP^{TOM+} neurons in males and females *CRFR1-GFP- AgRP^{TOM}* mice (n=3 for each sex) and in female *CRFR1-GFP- POMC^{TOM}* mice (n=2).

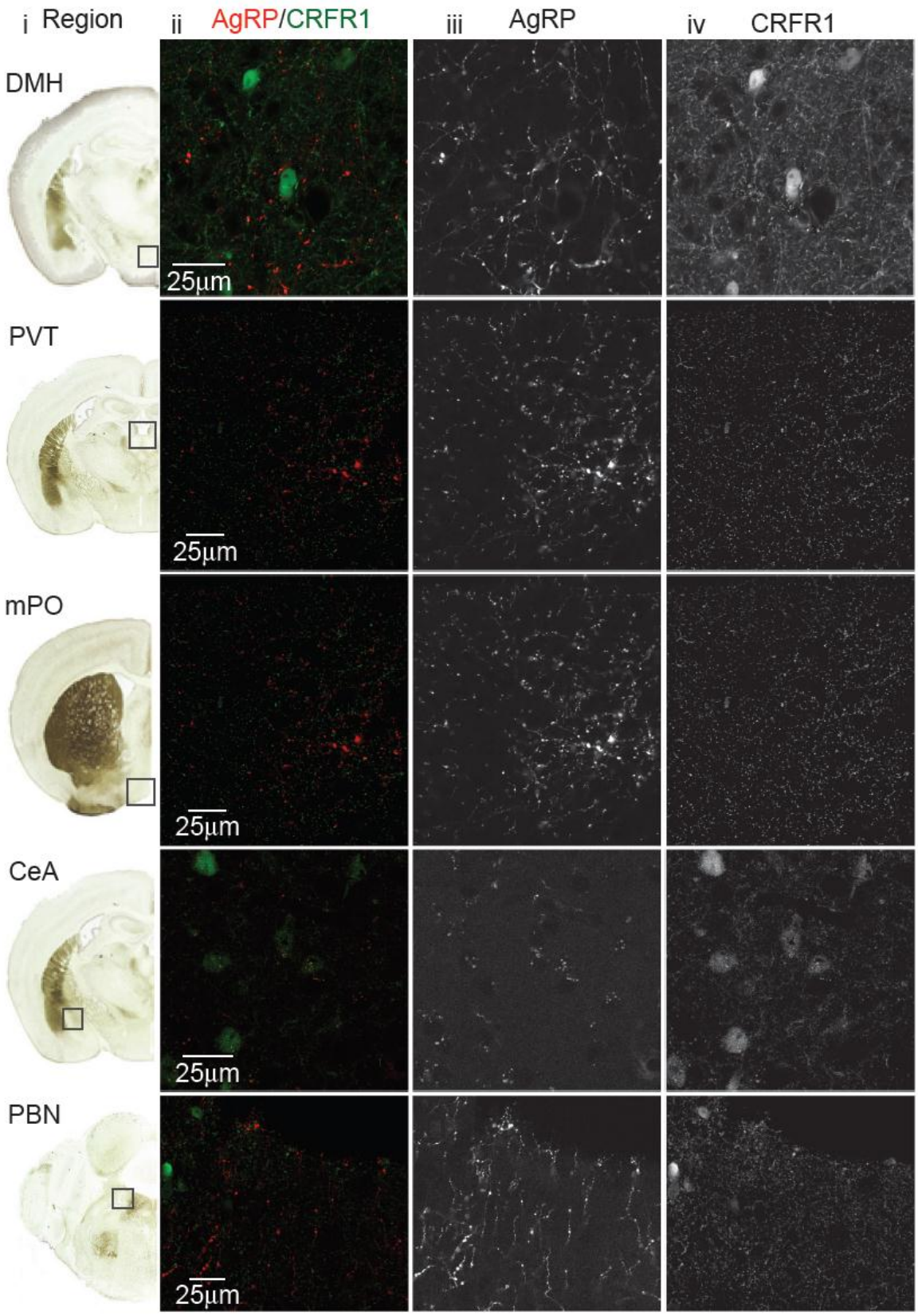
i Region
ii AgRP/CRFR1
iii AgRP
iv CRFR1
DMH
PVT
mPO
CeA
PBN
25μm
25μm
25μm
25μm
25μm

Figure S2. Projection mapping of AgRP^{+}CRFR1^{+} neurons. Related to Figure 3.

Nine known AGRP neuron projection fields were analyzed for AgRP^{+}GFP^{+} projections. (i) Brain coronal section adapted from the Paxinos & Franklin mouse brain atlas (Paxinos and Franklin, 2001), black box indicates region analyzed Black box indicates region analyzed. (ii) Overlaid images of AgRP^{TOM} fluorescence and GFP immunoreactivity. (iii) Tomato fluorescence reveals AgRP projections. (iv) GFP immunoreactivity in each region. See also Figure 3.

DMH- dorsomedial hypothalamus, PVT- paraventricular nucleus of thalamus, mPO- medial preoptic area, CeA- central amygdala, PBN- parabrachial nucleus. Scale bar, 25 μm.

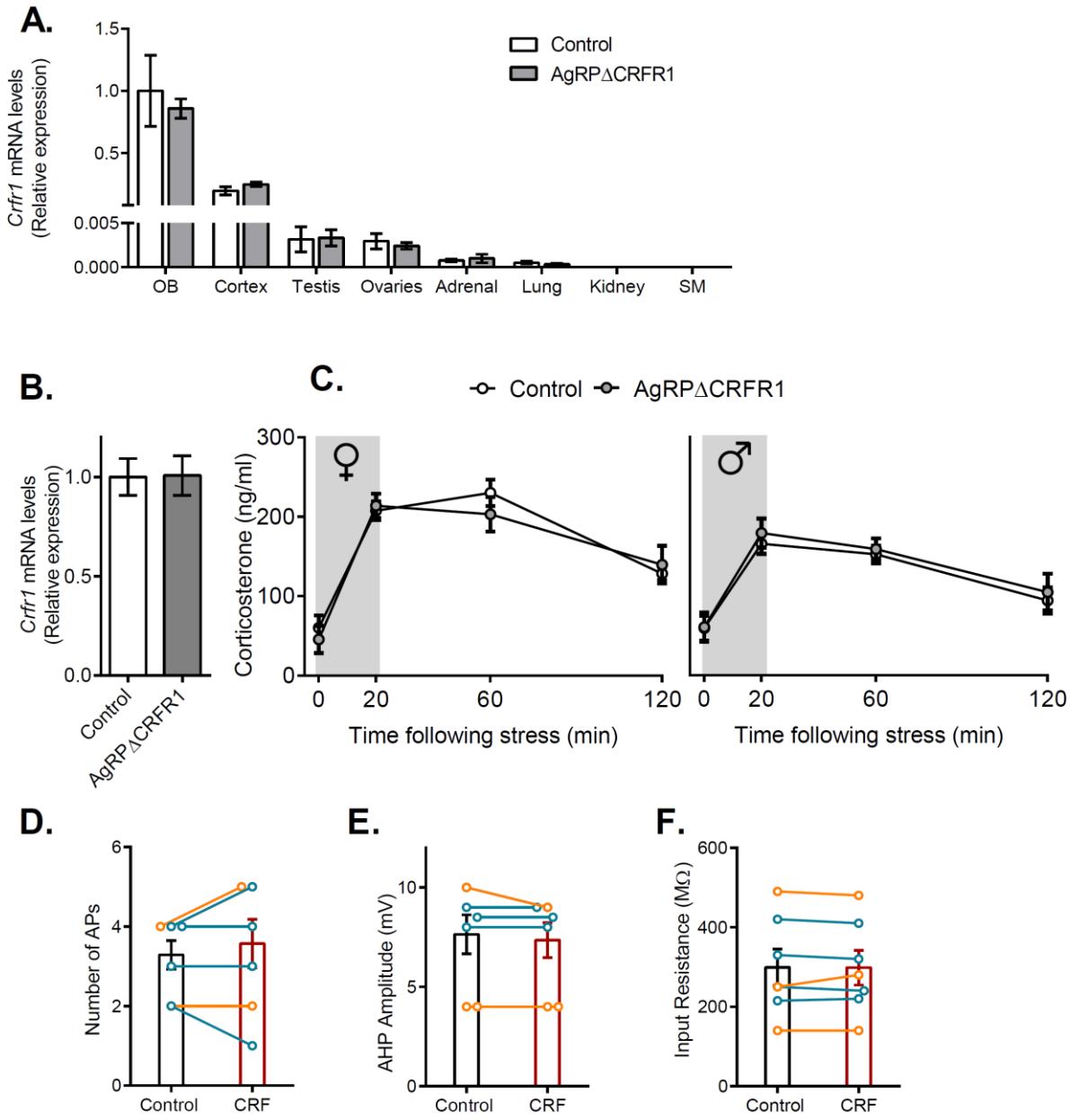

Figure S3. Unaltered HPA function in AgRPΔCRFR1 mice. Related to Figure 4.

A. *Crfr1* expression in several brain regions and peripheral tissues in AgRPΔCRFR1 mice and their control littermates (n=6).

B. Pituitary *Crfr1* expression in AgRPΔCRFR1 mice and their control littermates (n=5-6). Data are shown as mean ± SEM.

C. Basal and stress induced HPA function in females (left; n=8) and males (right; n=8-9) AgRPΔCRFR1 mice. Gray rectangle represents restraint time. Data are shown as mean±SEM.

D-F. CRF has no effect on AgRP neurons which do not express CRFR1. All parameters tested, firing rate (D), AHP amplitude (E), and R_{in} (F) remain constant in the presence of CRF (125nM; n=7 neurons). Each single experiment is represented with blue (female) or orange (male) circles and the histogram the mean ± SEM.

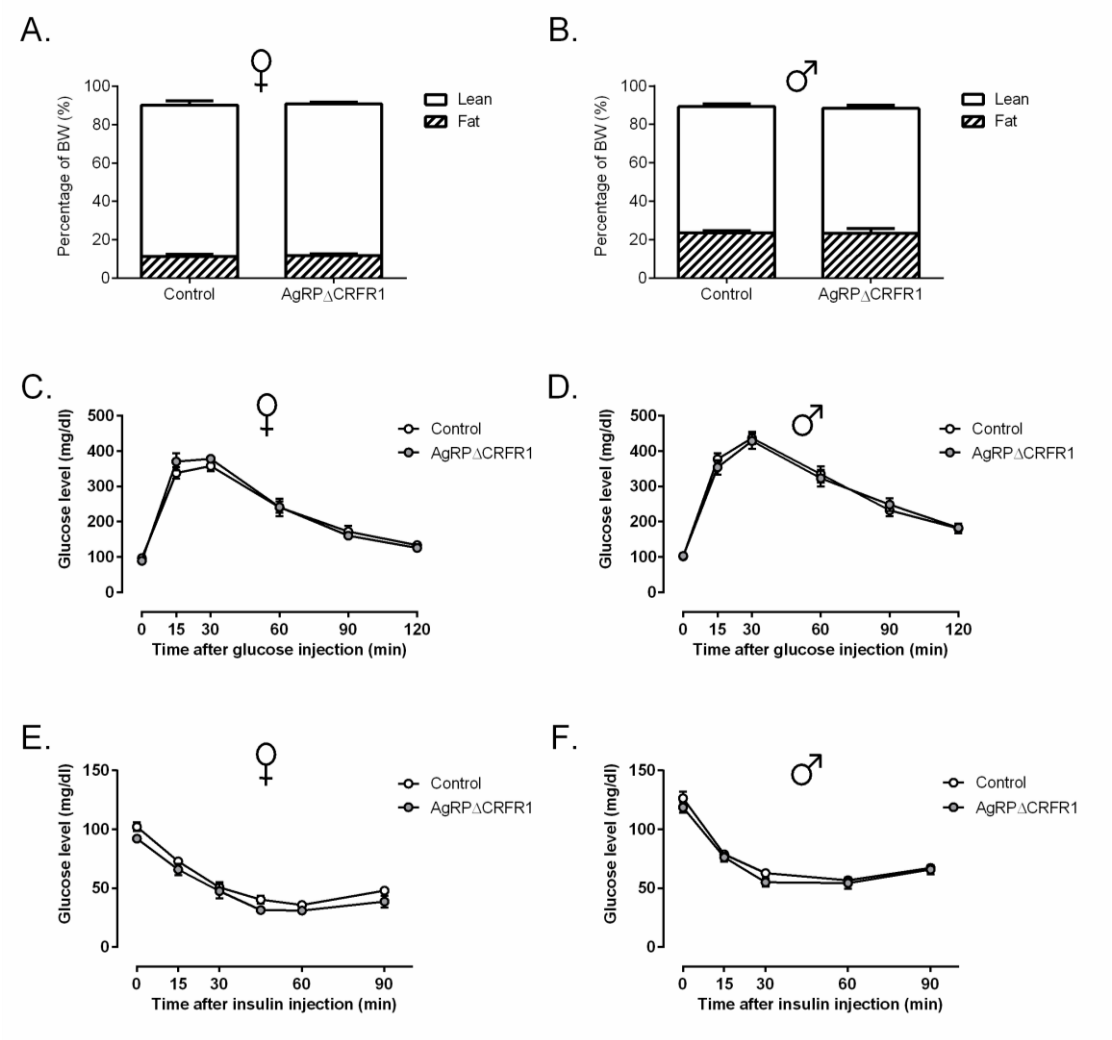

Figure S4. Unaltered body composition and glucose homeostasis in AgRPΔCRFR1 mice. Related to Figure 5.

A,B Body composition of females (A; n=6) and males (B; n=6-9) AgRPΔCRFR1 mice.

C-F Glucose and insulin tolerance tests in females (C,E; n=10, n=5-6) and males (D,F n=14-15; n=12-14) AgRPΔCRFR1 mice.

Data are shown as mean ± SEM.

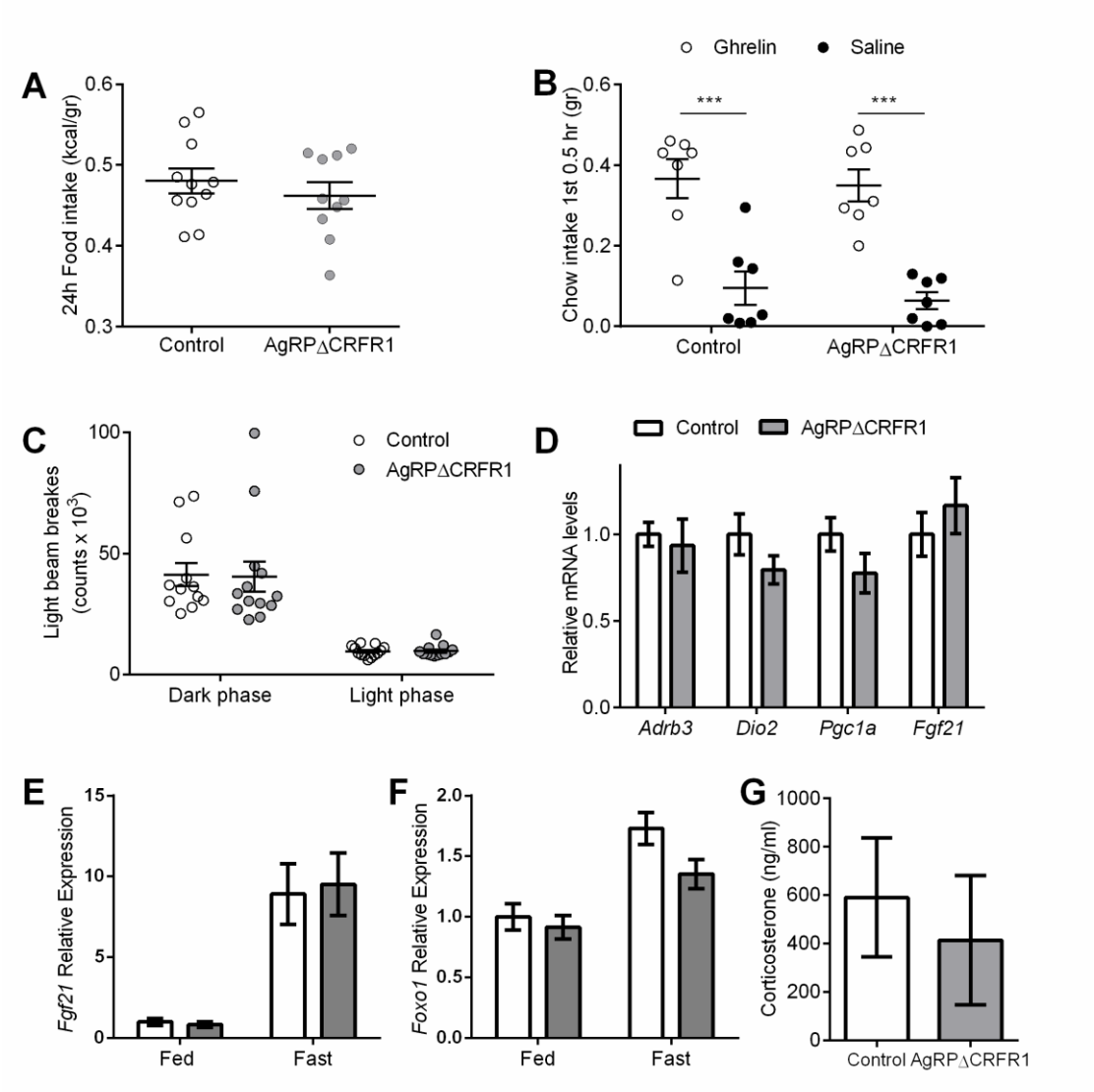

Figure S5. Phenotypes of AgRPΔCRFR1 female mice. Related to Figures 5 and 6.

A. Locomotor activity (n=11-13)

B. Food intake (n=10-11)

C. Food intake in 30min following ghrelin or saline injection (n=7)

D. Relative expression of selected genes in the BAT following exposure to 5°C (n=6-8).

E. Hepatic *Fgf21* relative expression at fast and fed state (n=7).

F. Hepatic *Foxo1* relative expression at fast and fed state (n=7).

G. Fasting corticosterone levels (n=4-5).

Data are shown as mean ± SEM. ∗p < 0.05.

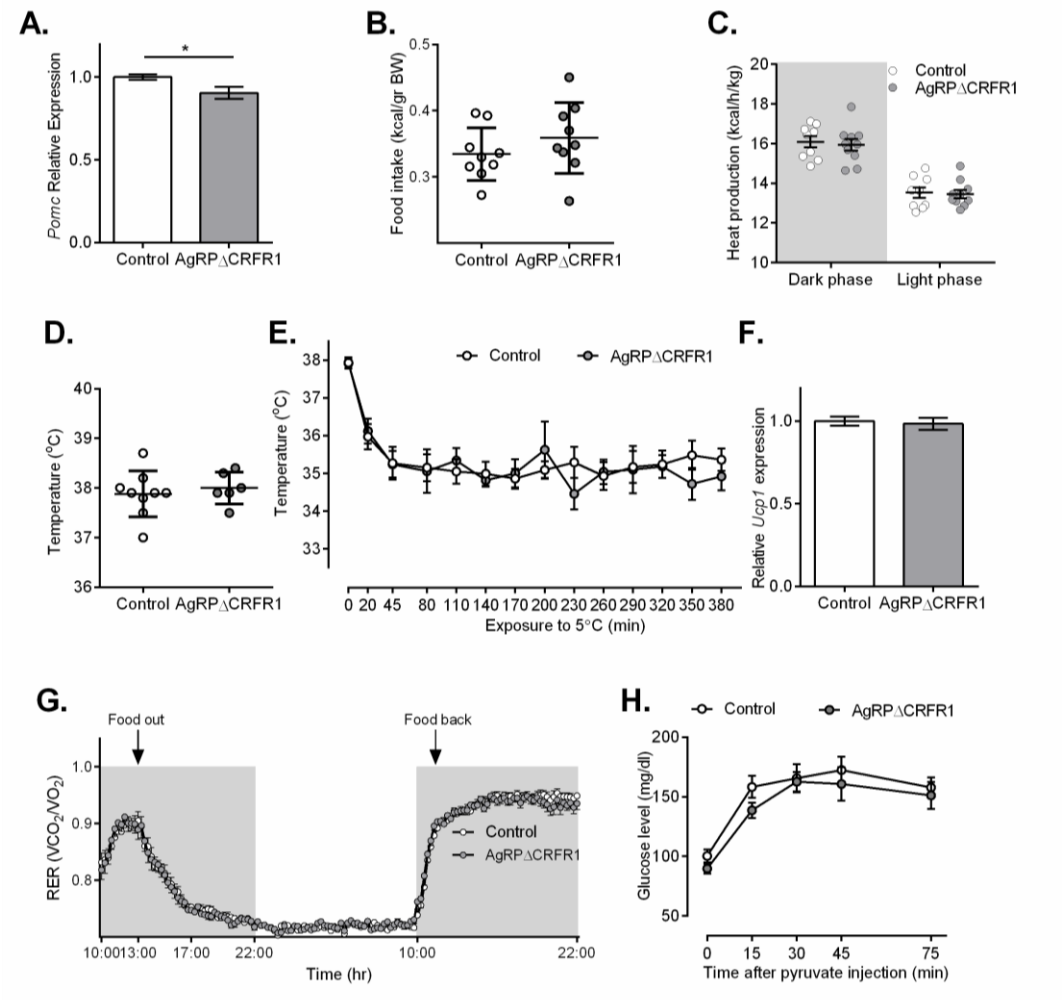

Figure S6. Phenotypes of AgRPΔCRFR1 male mice. Related to Figures 5 and 6

A. Relative *Pomc* expression in the mediobasal hypothalamus (n=5-6)

B. Food intake (n=9)

C. Heat production (n=9-10)

D. Body temperature (n=6-9).

E. Body temperature during cold challenge test (n=5-10).

F. Relative BAT *Ucp1* expression following exposure to 7h in 5°C (n=6-7).

G. RER kinetics during food deprivation and refeeding (n=11-13).

H. Glucose levels following pyruvate injection (2gr/kg; n=6-9)

Data are shown as mean ± SEM. *$p < 0.05$.

Supplemental Experimental procedures

Mice

CRFR1-GFP mice were kindly provided by the late Prof. Wylie Vale, Salk Institute, CA, USA. RIP-Cre mice (Postic et al., 1999) were kindly provided by Dr. Eran Hornstein, Weizmann Institute of Science, Israel.

The following lines were purchased from Jackson Laboratory (Bar Harbor, ME, USA): AgRP-IRES-Cre (Stock# 012899), POMC-Cre (Stock# 005965), CRF-IRES-Cre (Stock# 012704) and tdTomato reporter (Stock# 007909). To generate AgRP-conditional CRFR1 knockouts, AgRP-IRES-Cre mice had been backcrossed for four generations on a C57BL/6 background and then intercrossed with $CRFR1^{loxP/loxP}$ mice in which two loxP sites flank the second exon (Kuhne et al., 2012). Both experimental and control groups carried 2 floxed CRFR1 alleles, while only the experimental group carried the Cre allele. The genotyping reaction included the multiplex primer (Kuhne et al., 2012) which allows the detection of

AgRP-CRFR1−/− mice that show somatic recombination owing to stochastic embryonic expression of AgRP-IRES-Cre. These mice were excluded. Primers sequence will be sent upon request.

Stereotaxic injections

For immunostaining of secreted neuropeptides located in the axons terminals, mice were injected with colchicine which inhibits microtubule polymerization resulting in concentration of neuropeptides in the cell body. Colchicine (2µl of 1µg/µl) was injected to the lateral ventricles (injection coordinates: AP-0.22mm; ML+0.95mm; DV-2.2mm). Mice were sacrificed by perfusion when locomotor symptoms were observed.

For observation of synapses originated from PVN-CRF neurons, 300nl AAV9-CMV-Flex-synaptophysin-mCherry viral vector (McGovern Institute for Brain Research at MIT) were injected bilaterally into the PVN of *CRF-Cre* mice crossed with *CRFR1-GFP* mice (injection coordinates: AP-0.9mm; ML±0.3mm; DV-4.5mm). Mice were perfused 1 month following the injection.

Electrophysiology

Adult (6-to10 week-old) male and female mice were anaesthetized with isoflurane (Abbott, Abbott Park, IL, USA) and decapitated. The brain was gently removed from the skull and chilled in ice-cold choline chloride-based cutting solution containing (in mM): 120 choline chloride, 3 KCl, 27 $NaHCO_3$, 2 $MgCl_2$, 17 D-glucose, pH 7.4, saturated with carbogen (95% O_2/5% CO_2). The brain was trimmed in a large block containing the hypothalamus and afterwards sliced using a vibratome (HM650V, ThermoFisher Scientific, Waltham, MA). 300-µm-thick coronal slices were cut through the full extent of the arcuate nucleus/lateral hypothalamus. Slices were incubated for 45 min at 34°C in artificial cerebrospinal fluid

(ACSF), containing in mM: 125 NaCl, 2.5 KCl, 1.25 NaH_2PO_4, 25 $NaHCO_3$, 1 $MgCl_2$, 2 $CaCl_2$, and 25 Glucose, pH 7.3, saturated with carbogen. Subsequently slices were maintained in ACSF at room temperature (23–25 °C) for at least 60 min prior to patch-clamp recordings. ACSF contained 50 µM APV and 5µM NBQX to block ionotropic glutamate receptors.

All experiments were carried out at room temperature and slices were continuously superfused with ACSF containing 50 µM APV and 5 µM NBQX (4-5 ml/min). Neurons of the arcuate nucleus co-expressing AgRP-tdTomato and CRFR1-GFP, or AgRP-tdTomato alone, were visually identified by epifluorescence microscopy. After identification, the cell bodies of these neurons were visualized by infrared videomicroscopy and the gradient contrast system. Somatic whole-cell patch-clamp recordings (seal resistance >1GΩ) were performed in bridge mode using a discontinuous single-electrode voltage-clamp amplifier (SEC-10L, npi electronics, Tamm, Germany). Only measurements of the access resistance (R_a) were done in voltage-clamp mode (holding potential -70 mV). The current/potential was low-pass filtered at 3 kHz, digitized at 9 kHz via an ITC-16 interface and stored with the standard software Pulse 8.31 (HEKA Elektronik, Lambrecht/Pfalz, Germany). The patch-clamp electrodes (open-tip resistance 4-5 MΩ) were pulled from borosilicate glass capillaries (Harvard Apparatus, Kent, UK) on a DMZ-Universal puller (Zeitz-Instruments, Munich, Germany) and filled with a solution consisting of (in mM): 130 K-gluconate, 5 NaCl, 2 $MgCl_2$, 5 Glucose, 10 HEPES, 0.5 EGTA, 2 Mg-ATP, 0.3 Na-GTP, 20 phosphocreatine, pH 7.3 with KOH, osmolarity 305mOsm (all substances were from Sigma-Aldrich, St. Louis, MO).

5 min after reaching the whole-cell configuration, injection of 400-ms-long depolarizing current pulses was used to induce mild firing (1-6 action potentials) of the neurons. CRF (125 nM, Bachem, Bubendorf, Switzerland) was bath applied and the same current pulses were

applied again 15 min after starting CRF application. Due to CRF-independent fluctuations in the resting membrane potential (RMP), analysis of CRF effects on this parameter could not be performed. If such fluctuations occurred, we used continuous current injection to shift the RMP for the experiments in the presence of CRF to the control value.

Offline analysis was performed using the Pulse Software and statistical analysis with SigmaStat 3.5. Statistical comparisons were carried out using two-tailed paired t-tests with significance declared at $p<0.05$.

RNA preparation and quantitative-PCR

RNA was extracted from hypothalamic, mediobasal hypothalami (MBH), livers, adrenal glands, BAT or iWAT as indicated using miRNaesy mini kit (Qiagen Inc., Valencia, CA) according to the manufacturer's recommendations. RNA was extracted from olfactory bulb, cortex, testis, ovaries, lungs and skeletal muscle using TRIzol reagent (life Technologies Corp., Carlsbad, CA) according to the manufacturer's recommendations. RNA was reverse transcribed to generate cDNA using high capacity cDNA reverse transcription kit (Applied Biosystems Inc, Foster City, California). cDNA product corresponding to 10 ng RNA was used as templates for real-time PCR analysis.

Quantitative (q) PCR analysis was carried out using the StepOnePlus system using either SYBR Green or Taqman assays (Applied Biosystems, LifeTechnologies Corp., Carlsbad, CA). Primers were designed to span introns using Primer Express (Applied Biosystems, Carlsbad, CA). For The following TaqMan assays were used: mCRFR1–assay #Mm01240376_m1; mHPRT–assay #Mm01545399_m1. Primers sequence will be sent upon request.

In-situ hybridization

For detection of co-localization on single cell level, double ISH (DISH) was performed as previously described (Refojo et al., 2011). The following riboprobes were used: *Crfr1*, nucleotides 1728-2428 of GenBank accession no. NM_007762; *Gfp*, nucleotides 679-1396 of GenBank accession no. U55762. Specific DNA fragments coding for the riboprobes were generated by PCR applying T7 and T3 or SP6 primers using plasmids containing the above-mentioned cDNAs as templates. Antisense and sense cRNA probes were synthesized and labeled with 35^{S}UTP or dioxygenin (DIG) by in vitro transcription from 200 ng of respective PCR product used as templates. For DIG detection anti-DIG-POD (Fab) antibody was used 1:400. Tiramide-biotin signal amplification (TSA) was performed using the NEL700A Kit.

Glucose, insulin and pyruvate tolerance tests

GTT and ITT were performed as previously described (Chen et al., 2006). Briefly, following 5.5 h of fasting, glucose (2 g/kg body weight) or insulin (0.75 units/kg bodyweight, Sigma-Aldrich Co, St. Louis, MO, USA) were injected i.p. and glucose levels were measured at the indicated time points using an automatic glucometer (Roche Diagnostics). For pyruvate tolerance test, mice were fasted for 16 h before pyruvate injection (2 g/kg, Sigma-Aldrich Co).

Body composition

Mice body composition was assessed using EchoMRI-100TM (Echo Medical Systems, Houston, TX, USA).

Ghrelin and leptin injections

For assessing leptin-induced STAT3 phosphorylation, food deprived mice were perfused 1 hour following i.p. leptin injection (3μg/gr; PLR Ltd, Rehovot, Israel). For assessing ghrelin-induced neuronal activation, mice were perfused 1 hour following i.p. ghrelin injection (3μg/gr; kindly provided by the late Prof. Wylie Vale, Salk Institute, CA, USA).

Corticosterone measurement

For the evaluation of the endocrine response to stress, tail blood samples were collected before (basal), immediately after 20 minutes of restraint stress, and 80 and 120 minutes after stress initiation. Restraint stress was induced using a 50-mL ventilated conical tube. Plasma samples were immediately centrifuged and stored at −80°C until assays were conducted. Corticosterone concentrations were quantified using a corticosterone enzyme immunoassay kit (Cayman Chemical Co, Ann Harbor, Michigan, USA).

Ghrelin sensitivity test

Ghrelin (3 μg/gr) was injected i.p. into fed mice during the light phase and food intake was measured during 30 minutes. As control, similar volume of saline was injected on the subsequent day.

Supplemental References

Chen, A., Brar, B., Choi, C.S., Rousso, D.,Vaughan, J., Kuperman, Y., Kim, S.N., Donaldson, C., Smith, S.M., Jamieson, P., Li, C., Nagi, T.R., Shulman, G.I., Lee, K.F., and Vale, W. (2006). Urocortin 2 modulates glucose utilization and insulin sensitivity in skeletal muscle. Proc. Natl. Acad. Sci. U.S.A. *103*, 16580–16585.

Kuhne, C., Puk, O., Graw, J., Hrabe de Angelis, M., Schutz, G., Wurst, W., and Deussing, J.M. (2012). Visualizing corticotropin-releasing hormone receptor type 1 expression and neuronal connectivities in the mouse using a novel multifunctional allele. J. Comp. Neurol. *520*, 3150-3180.

Paxinos, G., and Franklin, K. B. J. (2001). The Mouse Brain in Stereotaxic Coordinates. Academic, San Diego.

Postic, C., Shiota, M., Niswender, K.D., Jetton, T.L., Chen, Y., Moates, J.M., Shelton, K.D., Lindner, J., Cherrington, A.D., and Magnuson, M.A. (1999). Dual roles for glucokinase in glucose homeostasis as determined by liver and pancreatic beta cell-specific gene knock-outs using Cre recombinase. J. Biol. Chem. *274*, 305-315.

Refojo, D., Schweizer, M., Kuehne, C., Ehrenberg, S., Thoeringer, C., Vogl, A.M., Dedic, N., Schumacher, M., von Wolff, G., Avrabos, C., *et al.* (2011). Glutamatergic and dopaminergic neurons mediate anxiogenic and anxiolytic effects of CRHR1. Science *333*, 1903-1907.